Enhanced performance of a PtCo recombination catalyst for reducing the H_2 concentration in the O_2 stream of a PEM electrolysis cell in the presence of a thin membrane and a high differential pressure

*N. Briguglio, F. Pantò, S. Siracusano, A. S. Aricò**

CNR-ITAE Institute of Advanced Energy Technologies, National Research Council

Via Salita S. Lucia sopra Contesse 5, 98126 Messina, Italy

**Corresponding author: Tel.: +39 090 624237. E-mail address: arico@itae.cnr.it*

Abstract

High electrochemical efficiency at elevated current densities and low H_2 concentration in O_2 can be achieved in PEM electrolysis using thin membrane and integrated recombination catalyst. An enhanced PtCo alloy recombination catalyst was synthesized and used at the anode of a membrane-electrode assembly (MEA). This allowed reducing the H_2 concentration in the oxygen stream during electrolysis operation with a thin 50 µm perfluorosulfonic acid (PFSA) Aquivion® membrane. Both dual-layer and composite anode configurations (PtCo/IrRuOx) were investigated. The electrochemical performance of the MEAs containing the recombination catalyst was better than a bare MEA while producing a decrease of the H_2 content at the anode. This allowed extending the partial load operation down to 5% at 55°C under a differential pressure of 20 bar. The effects of the cathodic pressure and cell temperature (including evaluation of intermediate temperature operation at 140 °C) on both electrochemical performance and H_2 concentration in the anode stream were investigated. An excellent performance of 4 A cm^{-2} at 1.75 V, at 140 °C, 20 bar cathode pressure, 5.5 bar anode pressure, with 0.6 mg cm^{-2} overall precious metal catalysts content was recorded. At 140 °C, the MEA also showed a moderate H_2 concentration in O_2 of about 2.3 %, almost constant through most of the current density range.

1. Introduction

Hydrogen produced by electrolysis has recently gained significant attention as energy carrier to store the excess of electricity produced by renewable energy sources that can not be fed into the grid. [1–4]. The storage of hydrogen at high volumetric energy density, e.g. as liquid (cryogenic) hydrogen, requires large energy consumption and technical safety assessment. Instead, the approach of a direct production of pressurized hydrogen from electrolytic water splitting appears very attractive. This can allow saving relevant amounts of energy being the electrochemical compression, according to the Nernst law, much more efficient than the mechanical gas compression. The latter is consuming about 20% of the overall energy involved in the transformation cycle from liquid water to hydrogen gas pressurised at about 700 bar as needed for refuelling modern fuel cell vehicles [4]. Polymer electrolyte membrane (PEM) electrolysers are in principle able to produce hydrogen at very high pressure thus reducing the post-compression energy consumption. These systems are also relatively compact since they operate at high current density and are characterised by proper dynamic behaviour for grid-balancing service and direct interface with renewable power sources [4–10].

One of the main factors limiting the efficiency of PEM electrolysers is that at high current density e.g. 3 A cm^{-2} (corresponding to high production rates), ohmic losses dominate the overall behaviour with about 85% of polarisation losses [11]. These losses are mainly associated to the use of thick perfluorosulfonic acid (PFSA) membranes, like Nafion® 117 membrane. Thick membranes are used to provide a barrier to H_2 crossover under high-pressure operation avoiding formation of explosive mixtures at the anode compartment.

On the other hand, a thin membrane can reduce the ohmic resistance of an electrolysis system allowing to increase the current density at a specific voltage efficiency. This allows

a decrease of capital costs which are inversely related to the hydrogen production rate [11].

However, the voltage efficiency (ratio between thermoneutral potential and cell voltage) decreases by increasing the current density as more heat is released into the atmosphere by the electrolysis system [12]. Alternatively, at nominal operating current density, a thin membrane would result in a decrease of ohmic losses thus increasing the voltage efficiency. The cost of green electrolytic hydrogen production is affected by both the capital costs of the electrolysis system (CAPEX) and operating costs (OPEX). The OPEX impact is mainly related to the renewable electricity cost. Thus, an increase of the process efficiency is highly desirable.

Gas permeability in the PFSA membranes is largely related to membrane thickness, permeability and operating temperature [13–19]. Thin membranes cause a large increase of gas crossover especially when the cell operates under asymmetric (differential) pressure conditions and at high temperature [1, 18].

In several commercial PEM electrolysers, the cathode compartment is pressurized whereas the anode stream is kept at ambient pressure. This avoids the oxidation of the current collectors made in titanium and increases the safety conditions (fire and explosion hazards are amplified by the presence of pressurised oxygen). An asymmetric working pressure of 30-40 bar is considered a trade-off between the need to pressurise hydrogen and the technological requirements (e.g. in terms of design and sealing) [20].

The effects of hydrogen permeation towards the anode are mostly evident at low partial loads (below 20%) [19, 21]. When the current density is low, the dilution effect by the produced oxygen is also small and the hydrogen concentration in the oxygen stream is high [22,23]. For safety reasons, an electrolysis system is shutdown when the hydrogen concentration in oxygen reaches 2-3 % [3,24,25,26]. Commercial PEM electrolysers

usually consist of a thick (170 µm) Nafion 117 membrane separator to offer a physical barrier to hydrogen permeation at high pressure [27,28]. A reduction of the membrane thickness can provide a simple and effective option to increase the current density and reduce the capital costs. However, this approach requires, in parallel, a mitigation strategy to minimize the hydrogen concentration in the oxygen stream, especially at low partial loads.

In the literature, several reports have addressed a better comprehension of hydrogen crossover and related issues [15–17,29–31]. With regard to oxygen permeation to the cathode, an external catalytic gas recombiner (deoxigenation catalytic recombiner or deoxo) converting the traces of permeated oxygen into water through a H_2/O_2 recombination process [32, 33]

To mitigate the hydrogen crossover, the strategies developed until now have been based on the modification of membrane structure by the use of Pt nanoparticles, specific fillers or nanofibrous reinforcements [34–36]. The use of a Pt electrode layer in between two membranes has also been reported in literature [37,38, 39].

The present study instead explores the concept of a recombination catalyst similar to that used in a deoxo system but integrated in a membrane-electrode assembly (MEA). In particular, the recombiner is used inside the anode where permeated hydrogen meets evolved oxygen. To avoid flammability occurrence in PEM electrolysers, the recombiner characteristics and operating conditions are essentially different from those of a conventional Pd/Al_2O_3 catalyst used in a deoxo system for purification purposes. The latter operates in the context of a chemical process occurring inside a packed bed reactor that is fed with a hydrogen stream containing traces of oxygen. Whereas, for the recombination catalyst integrated in the MEA, beside a good activity, other requisites are needed. These regard a proper electronic conductivity, a good capability to sustain oxidising conditions (a

reducing environment is instead occurring for the hydrogen stream passing through the deoxo) and the need to avoid interfering with the oxygen evolution.

In this study, we show the progress achieved in comparison to our previous work where a Pt-alloy catalyst was integrated in the anode of an electrolysis MEA and investigated as hydrogen oxidation catalyst [40]. The present advances deal with both catalyst properties and MEA configuration. Moreover, a PEM electrolyser operation at intermediate temperatures (140°C) under pressurised conditions was explored because of the enhanced reactions kinetics and lower cooling requirements.

In a previous work [40], a Pt-Co alloy was deposited over an Aquivion® perfluorosulfonic membrane (90 µm) forming thus an interlayer between the membrane and a conventional IrRuOx anode catalyst layer deposited on the outer surface of the Pt-alloy. Ir-oxide based catalysts are widely used for the oxygen evolution in PEM electrolysis [41–47]. Our previous study showed promising activity of the PtCo catalyst in reducing the hydrogen content in an oxygen stream especially when this was investigated out-of-cell in a gas-phase packed-bed catalytic reactor (99.5%) [40]. However, a lower performance was recorded when the oxidation catalyst was integrated in the membrane-electrode assembly. This was attributed to the prevalence of an electrochemical oxidation mechanism for the permeated hydrogen compared to the pure recombination mechanism of H_2 and O_2 into water that occurred in the catalytic packed bed reactor. Based on the previous results, the aim of the present study was to improve the catalyst properties in relation to the recombination process and its integration in the MEA. In particular, to exploit better the PtCo catalyst's functionality, this was mixed with a conventional IrRuOx catalyst and deposited over the membrane to form a composite anode layer (MEA: cathode/membrane/mixed IrRuOx-PtCo anode). This configuration was compared with the previous configuration where the PtCo alloy was allocated in between the membrane and

the IrRuOx oxygen evolving layer forming a double layer anode (MEA: cathode/membrane/ PtCo hydrogen oxidation layer/ IrRuOx oxygen evolving layer).

The nanosized PtCo catalyst used for both the composite (mixed) and double layer (unmixed) anode was an improved version of our previous unsupported PtCo alloy [40]. In particular, a different preparation procedure was used to obtain a catalyst with larger degree of alloying between Pt and Co and a smaller crystallite size.

Moreover, the properties of PtCo for reducing the hydrogen concentration in the anodic steam were assessed in the presence of a thinner PFSA membrane (50 μm) characterised by larger gas permeation rate compared to the membranes used in our previous works (90 μm) [47]. This allowed to assess the catalytic system under more harsh operating conditions as well as to explore the possibility of using thin polymer electrolyte membranes in PEM electrolysis as a useful approach to reduce ohmic losses and enhance the voltage efficiency.

2. Experimental

2.1. Materials

The new recombination catalyst here synthesized was a nanosized unsupported Pt-Co alloy (85:15 at. %). The synthesis of the catalyst was carried out according to the sulphite complex route [40]. Platinum and cobalt sulphite precursors, in the selected stoichiometric amounts, were neutralised with sodium hydroxide and then oxidised with hydrogen peroxide. The solution was stirred overnight and the pH was adjusted with sodium hydroxide. Colloid formation and successive solid precipitation occurred upon heating the solution at 70° C. The obtained amorphous oxides mixture was then washed, filtered and dried in air at room temperature. The post-synthesis treatments consisted of a reduction

step, in order to promote the alloy formation, and a pre-leaching process, in order to remove both impurities and unalloyed Co atoms from the surface of the catalyst. With respect to our previous Pt-Co alloys [40], in this work, a lower reduction temperature and an acidic pre-leaching treatment, in a solution five times more concentrated than the previous one were used. These conditions were selected after an optimisation procedure, in order to obtain a Pt-Co catalyst with smaller crystallite size and lower content of unalloyed Co species. The catalyst was reduced in diluted hydrogen (10% vol. H_2 in helium at 150 °C). Thereafter, it was pre-leached in 0.5 M perchloric acid at 80° C. The catalyst was finally milled at 300 rpm to improve its morphology for the spray deposition process during the MEA manufacturing.

3.2 Physico-chemical characterisations

The structural analysis was performed by using a Philips X-Pert diffractometer equipped with a CuKα as radiation source. The diffraction patterns were interpreted by means of the Joint Committee on Powder Diffraction Standards (JCPDS).

The morphology was investigated by scanning electron microscopy (SEM) and transmission electron microscopy (TEM). SEM was carried out by a FEI S-FEG XL30 microscope equipped with energy dispersive X-ray (EDX) spectrometer, in order to quantify the bulk elemental composition. Transmission electron microscopy (TEM) was performed with a FEI CM12 microscope; catalysts were dispersed in isopropyl alcohol and deposited on a carbon-coated copper grid.

The surface composition was obtained through an X-ray photoelectron spectroscopy analysis by using a PHI 5800-01 spectrometer. Spectra were collected using a monochromatic Al Ka X-ray source and acquired with a pass energy of 187.85 eV for survey and 11.75 eV for high resolution spectra, respectively.

2.2. *Preparation of catalyst-coated membrane*

Membrane-electrode assemblies were prepared by using the catalyst-coated membrane (CCM) approach. The specific properties of the electrocatalysts are reported in Table S1 (supporting information) along with the corresponding bulk and surface composition, the crystallographic structure and crystallite size. The characteristics of the Pt/C hydrogen evolution catalyst are described in Fig. S1 whereas those of the $IrRuO_x$ oxygen evolution catalyst are presented in Fig. S2. These catalysts are essentially similar to those reported in previous papers [40-42].

A commercially available melt-extruded membrane Solvay Aquivion® membrane (E98-05S) with an equivalent weight (EW) of 980 g eq^{-1} and a thickness of 50 µm was used as membrane separator. A 40% Pt/C (Ketjenblack® carbon) was used for hydrogen evolution whereas $IrRuO_x$ (70:30 at.) was used as anode catalyst for oxygen evolution (Figs. S2 and S3, supporting information). The Aquivion® ionomer dispersion (D98-06AS), used for the electrode manufacturing, had similar structure and composition of the membrane.

The catalyst-ionomer inks were prepared in order to obtain, after drying, 85 wt. % of $IrRuO_x$ catalyst with 15 wt. % of ionomer and 72 wt. % of Pt/C catalyst with 28 wt. % of ionomer, respectively. The cathode ink was in all cases spray coated onto the membrane. In the bare MEA, i.e. a MEA not containing any PtCo recombiner, the IrRuOx anode ink was coated onto the other membrane side. Whereas, in the presence of the recombination catalyst, different approaches were used for the anode manufacturing (see below).

The metal loadings for the bare MEA were 0.3 mg Ir + Ru cm^{-2} for the $IrRuO_x$ catalyst and 0.1 mg Pt cm^{-2} for the Pt/C catalyst.

The activity of the PtCo catalyst for reducing the hydrogen concentration in the anode stream was investigated using two different configurations: “mixed” and “unmixed”

configurations referring to a composite anode catalyst layer made of IrRuOx and PtCo or a dual-layer anode with PtCo in between the membrane and the IrRu-oxide layer, respectively (Fig.1).

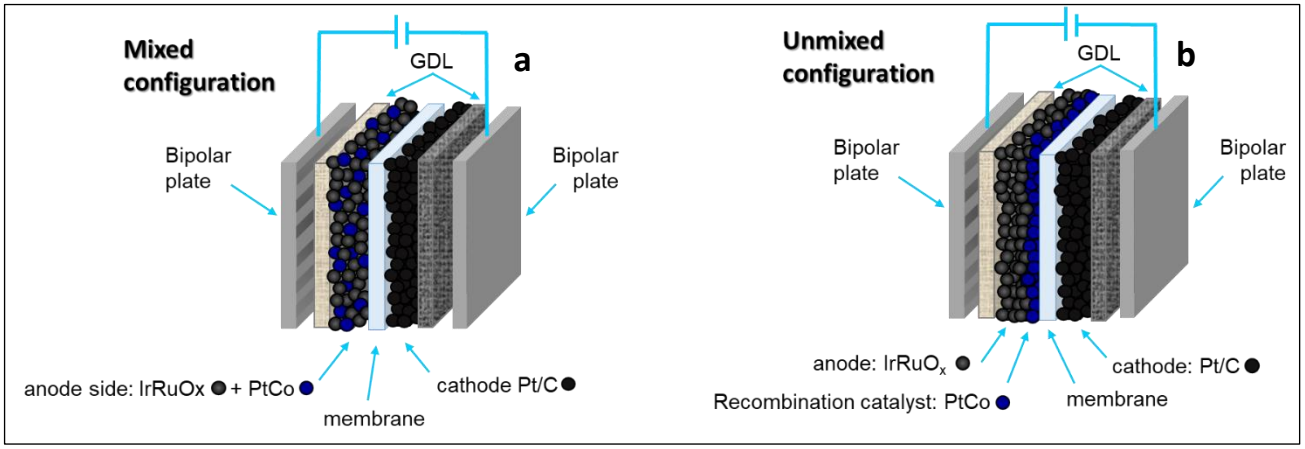

*Fig. 1. Structure of the MEAs based on the $Pt_{5.6}Co_1$ recombination catalyst: "mixed" (**a**) and "unmixed" configuration (**b**).*

In the unmixed configuration, the recombination catalyst ink consisting of 85% wt. PtCo and of 15% wt. ionomer was directly sprayed onto the membrane. Subsequently, the anode layer made of 85 wt. % of $IrRuO_x$ catalyst and 15 wt. % of ionomer was deposited onto the outer surface of the PtCo layer.

The metal loadings for the unmixed configuration were 0.3 mg Ir + Ru cm^{-2} for the $IrRuO_x$ catalyst, 0.2 mg Pt cm^{-2} for the PtCo catalyst at the anode and 0.1 mg Pt cm^{-2} for the Pt/C cathode catalyst.

In the mixed configuration, the recombination catalyst was mixed in a proper amount with the IrRuOx anode catalyst and the ionomer. The mixed (composite) ink consisting of 85% wt. catalyst and 15% wt. ionomer was spray coated onto the membrane. The metal loadings for the mixed configuration were 0.3 mg Ir + Ru cm^{-2} for the $IrRuO_x$ catalyst, 0.2

mg Pt cm^{-2} for the PtCo catalyst at the anode and 0.1 mg Pt cm^{-2} for the Pt/C cathode catalyst.

A carbon based gas diffusion layer (GDL ELAT from ETEK) was attached to the cathode side of the CCMs. The assemblies were hot-pressed for 1.5 min at 190 °C and 6 kN to favour the adhesion of the catalytic layers to the membrane. This occurred at a temperature higher than the glass transition temperature of the Aquivion® polymeric membrane (160 °C) [18, 42]. The active area (geometrical electrode area) of the MEAs was 8 cm^2. After the hot-pressing procedure, the membrane-electrode assembly with carbon GDL attached to the cathode, was physically contained between two dense Ti felts. These primarily acted as mechanical support for the MEA. Moreover, the felt at the anode acted as diffusion layer for oxygen evolution. These assemblies were installed in the PEM single cell.

2.3. Electrochemical measurements

Electrochemical measurements were carried out using an in-house developed single cell test station for high differential pressure electrolysis operation equipped with high pressure ITM Power (UK) single cell test fixture and a Varian micro gas-chromatograph for the determination the hydrogen concentration in the oxygen stream at the anode (Fig. S3 supporting information). The single cell electrolysis performance was evaluated at different pressures (atmospheric, 5, 10 and 20 bar) and temperatures (55°, 90° and 140 °C). The determination of the hydrogen crossover was carried out under differential pressure i.e. pressurised hydrogen and non-pressurised oxygen at 55°, 90°C. Thus, the pressure values reported under these conditions are referred to the cathodic compartment only, since the anodic compartment was not pressurised at 55 °and 90 °C. At 140 °C, it was necessary to keep constant the anode compartment pressure at 5.5 bar whereas the cathode pressure was varied as in the experiments at lower temperature.

Deionised water (<0.1 μS), further purified by an ion exchange resin cartridge, was supplied by a pump at a flow rate of 1 ml min^{-1} cm^{-2} to the anode compartment. The temperature of the PEM single cell was maintained constant by monitoring the temperature of the recirculating water. This was heated at the specific operating temperature. To avoid water boiling at 140 °C, the anode compartment was pressurised. The water outlet was cooled down before being recirculated through the ion exchange resin.

A power supply (TDK GEN 25400-MD-3P400) was used to perform polarisation experiments in the galvanostatic mode by recording the cell voltage vs. the imposed current density.

An Autolab Metrohm potentiostat / galvanostat equipped with a 20 A current booster and a frequency response analyser (FRA) was used to perform electrochemical impedance spectroscopy (EIS). Electrochemical impedance analysis was carried out in the potentiostatic mode at 1.5 V and whenever possible also at 1.8 V. The frequency was varied from 100 kHz to 100 mHz in the single sine mode with a sinusoidal excitation signal of 10 mV pk-pk.

The activity of the PtCo catalyst was assessed by determining the hydrogen content in the anodic stream (the activity is inversely related to the H_2 concentration). The quantitative analysis of hydrogen concentration was performed at constant current density by an online micro gas-chromatograph (Varian Micro GC). The anodic gas stream was passed through a desiccator before being analysed.

3. Results and discussion

The main characteristics of the Pt/C and IrRuOx electrocatalysts used in the MEAs are reported in Table S1 and Figures S1 and S2 (supporting information). These materials

were already investigated in previous papers [47-48]. The focus of this work is essentially regarding the PtCo catalytic recombiner.

3.1 Microstructure and morphology of the unsupported PtCo recombination catalyst

The atomic ratio for the PtCo alloy was investigated by EDX measurements. With respect to the PtCo catalyst reported in a previous study [40], a different preparation procedure was used. This provided enhanced catalyst properties in terms of small crystalline size and better alloying between Pt and Co [49]. In effect, the unalloyed Co species were removed through a strong pre-leaching treatment in acid. A bulk composition of 85:15 at. % of Pt:Co was obtained after an optimisation of the post-synthesis treatments (Fig. S4 supplementary information). A lower reduction temperature and a pre-leaching treatment in an acidic solution five times more concentrated than that previously used [40] were adopted. The aim was to achieve a platinum enrichment on the surface to improve the stability of the catalyst under anodic operating conditions.

Fig. 2 shows the occurrence of a face-centered cubic crystallographic structure of Platinum (JCPDS card no. 4-802) for the PtCo catalyst. The peaks show a significant shift towards higher Bragg angles with respect to the diffraction pattern of platinum. The lattice constant for the PtCo alloy is determined from the inset in Fig. 2 (A_{220}=0.3865 nm). The corresponding estimated atomic content of Co in the alloy from the Vegard's law is about 15±2 % that is close to the nominal amount. No peaks related to other crystalline phases are detected for the catalyst. The average crystallite size as estimated by the Debye-Scherrer equation is 4 nm. A significant reduction of the crystallite size with respect to our previous recombination catalyst (around 10 nm) is observed.

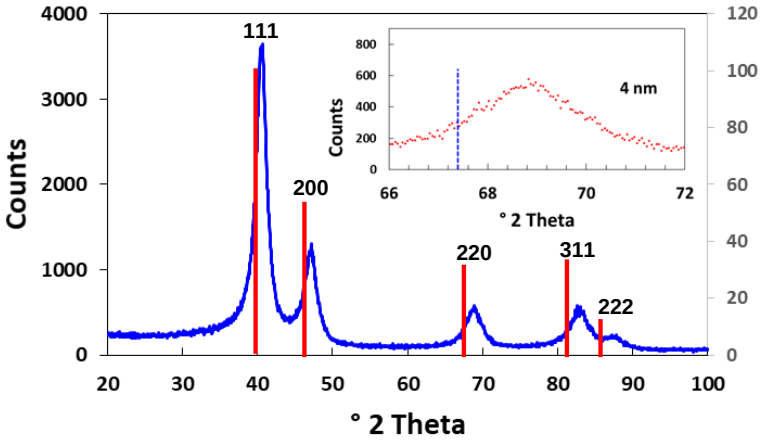

Fig. 2. X-ray diffraction patterns of $Pt_{5.6}Co_1$ catalyst and face centered cubic Pt as reference, JCPDS card no. 4-802. The inset shows the 220 peak broadening used for determining the mean crystallite size.

The morphology of the catalyst was investigated by SEM and TEM analyses. The SEM image in Fig. 3 shows a porous sponge-like morphology. The atomic ratio of platinum and cobalt in the alloy was studied at low magnification by EDX (Fig. S4). No impurities after the pre-leaching in perchloric acid were detected in the EDX spectrum (Fig. S4 supporting information). The inset in Fig. 3 relates to a TEM micrograph of the PtCo catalyst, which is composed by nanoparticles of spherical shape. The image depicts a relevant agglomeration that is a typically feature of unsupported catalysts. This does not allow to

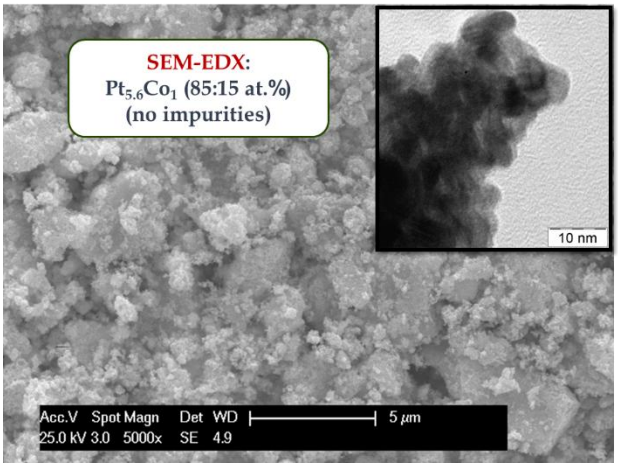

determining properly the particle size distribution.

Fig. 3. SEM and TEM (inset) micrographs of the PtCo catalyst.

3.2 Surface characterisation of the PtCo catalyst

The surface atomic composition of the PtCo recombination catalyst was investigated by XPS analysis. XP survey spectra of the pristine and sputtered $Pt_{5.6}Co_1$ catalyst (Fig. 4) revealed a prevailing occurrence of platinum on the surface, with a surface atomic composition of Pt:Co = 90:10.

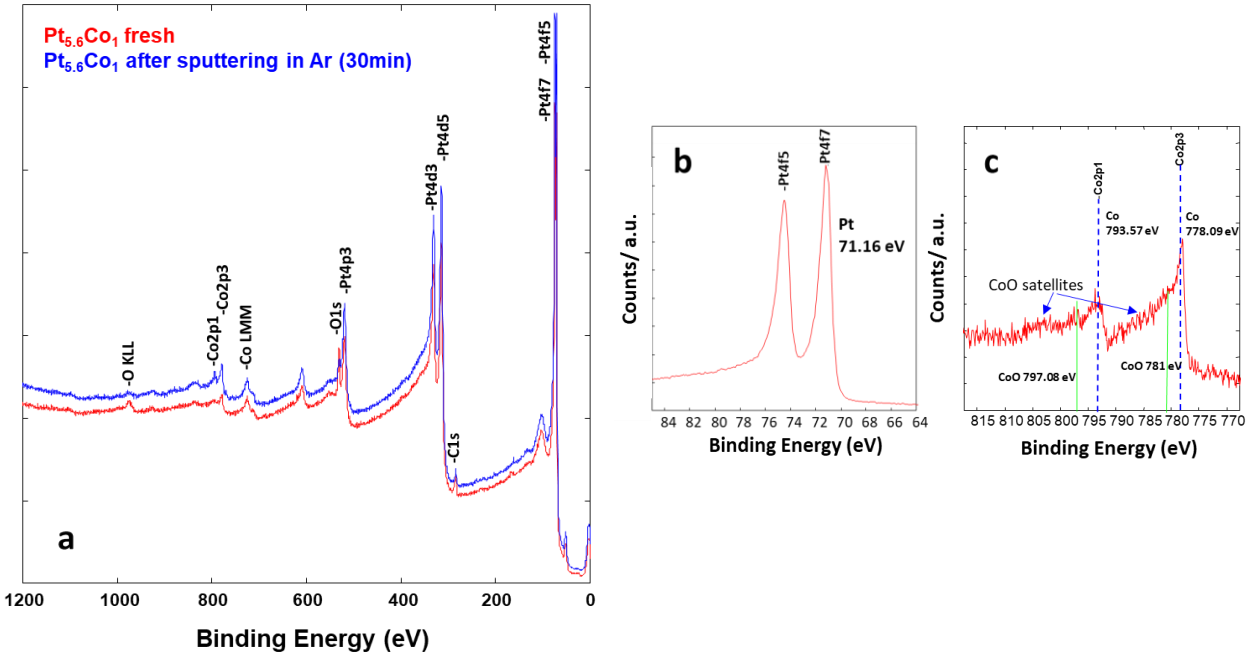

Fig. 4. Survey XP spectrum of the pristine and sputtered $Pt_{5.6}Co_1$ catalyst (a), high resolution XPS spectra of Pt 4f (b) and Co 2p (c).

After a sputtering treatment with argon ions at 5 kV for 30 min., the cobalt concentration on the surface increased reaching the EDX-determined bulk composition (Pt:Co = 85:15 $\%_{at}$). The O1s and C1s signals are related to adventitious carbon-containing species as

confirmed by a significant decrease of such signals after sputtering. High-resolution XPS spectra of the fresh catalyst show the prevailing occurrence of metallic Pt and Co on the surface. The contribution of cobalt oxide (CoO) to the overall Co2p spectrum was relatively low compared to metallic cobalt. The main peaks of CoO are indicated by full lines in Fig. 4c. Satellite peaks usually associated with the paramagnetic CoO are just slightly envisaged and are indicated by arrows (Fig. 4c). Thus, there is a slight presence of CoO but in a modest amount compared to metallic Co. The effect of Co in this catalyst is to favour a charge transfer to Pt. The surface properties of the IrRuOx catalyst is reported elsewhere [50]. Essentially, the catalyst is characterised by an enrichment of Ir on the surface.

3.3 Single cell electrochemical assessment of the Pt-Co alloy catalyst for the reduction of the hydrogen concentration in the oxygen stream

As reported in Fig.1,two different MEA structures (mixed and unmixed), based on the use of a PtCo recombination catalyst (RC) at the anode, were investigated. Fig. 5 shows a comparison of the H_2 content in the oxygen stream as function of the current density at a constant temperature of 55°C and at two different differential pressures (pressurised H_2, non-pressurised O_2) i.e. 10 and 20 bar. To evaluate the progress made in this work, the two configurations based on the present recombination catalyst and a thin 50 µm Aquivion (E98-05S) membrane were compared to an unmixed (double-layer anode) MEA based on a 90 µm Aquivion (E98-09S) membrane and containing our first version of a PtCo recombination catalyst [40]. The aim was to understand the enhanced activity of the present catalyst under more harsh conditions [49] determined by the presence of thinner membrane causing larger hydrogen crossover. At 55 °C, in all configurations, the H_2 concentration was relatively high at very low current densities (Fig. 5). However, it progressively decreased once the production of oxygen increased with the current density

and thus the permeated hydrogen at the anode was diluted. The lowest H_2 concentration in the oxygen stream was recorded, in the overall range of current density, for the MEA based on the present PtCo recombination catalyst (RC) mixed with the IrRuOx oxygen evolution catalyst. The H_2 concentration was kept below 2.5 % also at high differential pressure (20 bar) and at a low current density of 0.2 A cm^{-2} corresponding to 5% of partial load for an electrolysis system operating at a nominal current of 4 A cm^{-2}. It is interesting to observe that even using the unmixed approach, the new PtCo catalyst shows better capability to reduce the hydrogen concentration than the previously developed PtCo [40], under the same configuration (Fig. 5). This is evident under critical low load conditions (low current density) despite the smaller membrane thickness (50 vs 90 µm) of the present MEA and the consequently larger H_2 crossover compared to the previously developed MEAs. This was attributed to the smaller crystallite size and better degree of alloying of the present catalytic recombiner compared to our previous PtCo catalyst (see Fig. S5 support information). Moreover, it is worth mentioning that the $Pt4f_{7/2}$ binding energy for the present catalyst was 71.16 eV compared to 71.30 eV of the previously developed catalyst (Table S1, Fig. S8 support information). This indicates better metallic properties and larger charge transfer from Co to Pt for the present catalytic system. These characteristics make Pt sites on the surface less prompt to surface oxidation under electrolysis conditions. This property is fundamental for a more efficient adsorption of the permeated hydrogen molecules on the PtCo surface. The adsorbed molecules are thus oxidised to protons by effect of the high electrochemical potential or to water by the oxygen evolved at the neighbouring IrRuOx catalyst according to a chemical recombination process. The electrochemical oxidation of H_2 appears more effective in the unmixed (double layer anode) configuration; whereas, the mixed (composite catalyst layer) configuration should promote the direct recombination being the oxygen molecules evolved at the neighbouring catalytic sites.

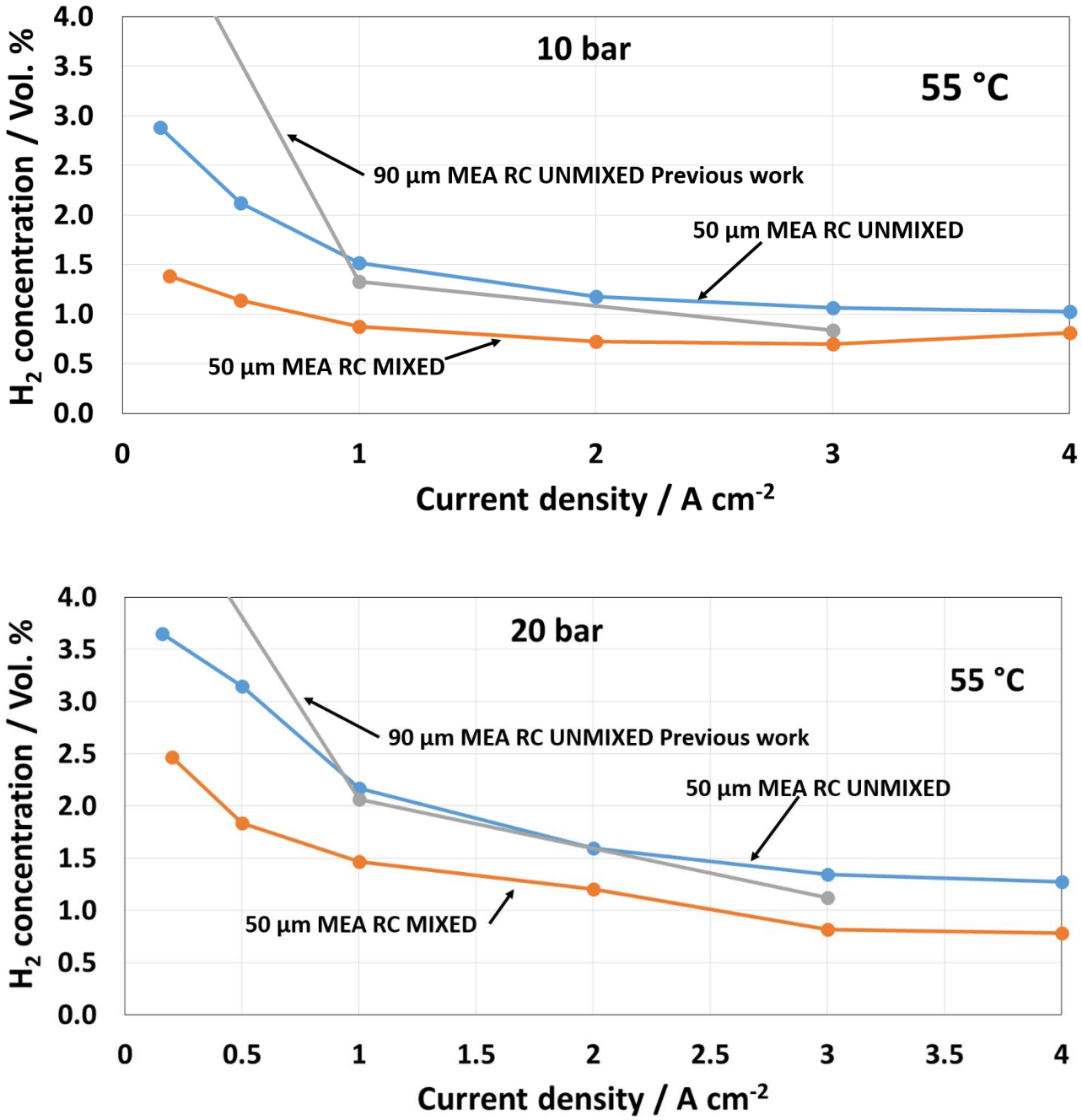

Fig. 5. H_2 concentration in the anodic oxygen stream at different current densities for various MEA configurations, at 55 °C, 10 and 20 bar differential pressure . RC refers to the PtCo recombination catalyst. Previous work refers to reference [40].

Fig. 6 shows a comparison of the polarisation curves for the different MEAs at 50 °C, 10 and 20 bar differential pressure. The electrochemical tests showed lower cell voltage at the same current density for the MEAs based on the unmixed configuration, both using the old and new version of recombination catalysts. It is clearly observed that the mixed

configuration, containing a composite anode catalyst layer, is characterized by a lower voltage efficiency compared to the two separate anodic layers. It is speculated that when the Pt sites are mixed to Ir and Ru catalytic sites, these can affect negatively the oxygen evolution reaction being Pt less active than Ir- and Ru-oxide. It is also noted that despite the different membrane thickness, the MEA based on the thin E98-05 membrane performs only slightly better at 10 bar and essentially similar at 20 bar compared to the MEA based on the thick E98-09 membrane. This may depend on the different membrane forming procedures causing slightly different protonic conductivity as well as to the MEA fabrication producing better mechanical compression in the case of the E98-09 membrane.

The mixed configuration appears superior to the unmixed approach in terms of reducing the concentration of hydrogen in the oxygen stream possibly due the different reaction mechanisms discussed above (chemical recombination vs. electrochemical oxidation). Moreover, the new PtCo catalyst allows reducing the H_2 content at the anode at the same extent of the previous PtCo system in the presence of a much thinner membrane (50 vs 90 microns) (Fig. 6).

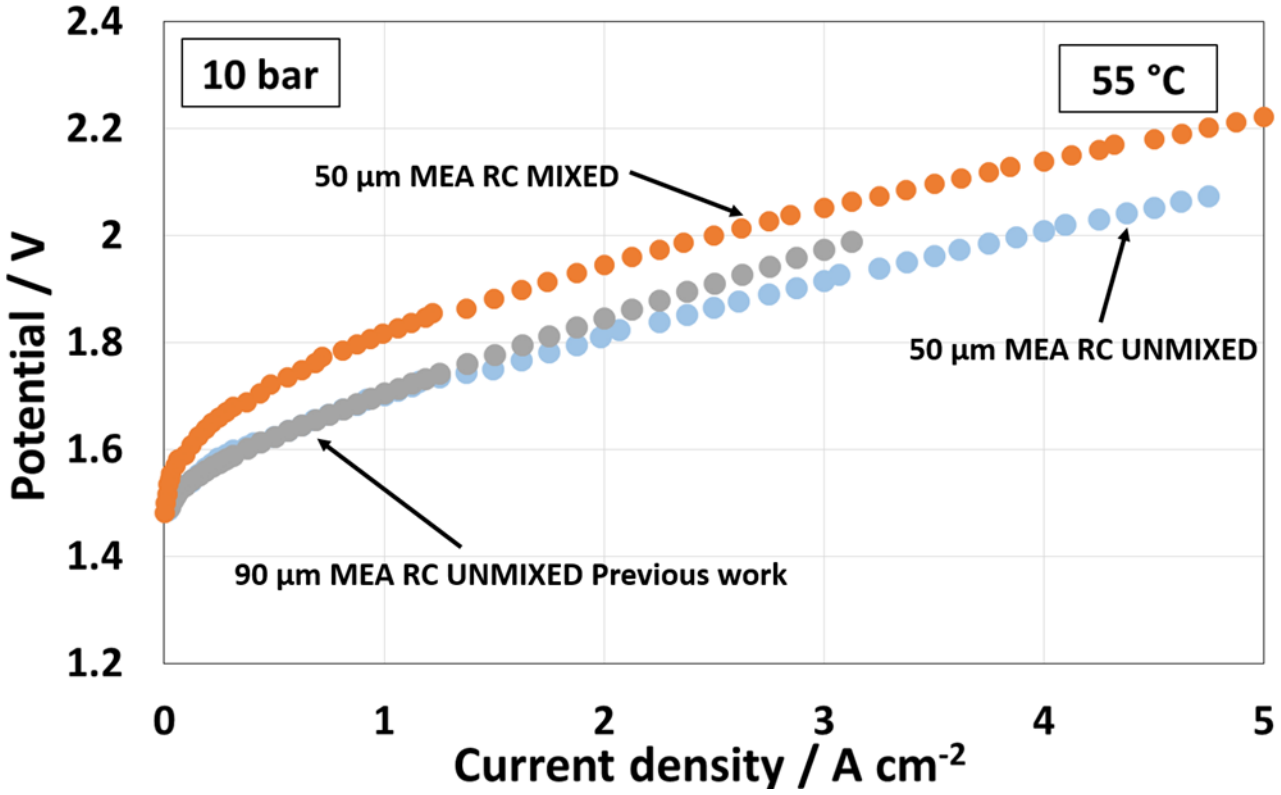

Fig. 6. Polarization curves for various MEA configurations, at 55 °C, 10 and 20 bar differential pressure . RC refers to the PtCo recombination catalyst. Previous work refers to reference [40].

Fig. 7 shows a comparison at 90°C between the mixed and unmixed configurations in terms of electrochemical performance (Fig. 7a) and activity for reducing the hydrogen concentration (Fig. 7b) at the anode. Also at 90°C, the PtCo catalyst in the mixed configuration shows a lower electrochemical performance than the unmixed one. The H_2 concentration in O_2 was still lower for the recombination catalyst mixed configuration (as observed at 55 °C). The RC unmixed configuration showed interesting electrochemical performance at 20 bar and 90°C (~1.87 V at 4 A cm^{-2}) but relatively high H_2 concentration in O_2 at low current density (Fig. 7). The H_2 concentration in O_2 was relatively high at 20 bar and 90°C, about 3.3 % at 1 A cm^2, for the thin 50 µm Aquivion® membrane equipped with the catalytic recombiner in the dual layer anode (Fig. 7). Thus, for the latter configuration operating with a nominal operating current density of 4 A cm^{-2}, the minimum applicable load is about 25%. Whereas, if the mixed configuration is preferred (Fig. 7),

assuming, also in this case, a nominal operating current density of 4 A cm^{-2}, as a proper compromise between efficiency and production rate, the minimum partial load operation can be as low as 5% (0.2 A cm^{-2}). This can provide a significant improvement of the dynamic behaviour of thin-membrane based electrolysers with just a slight loss of voltage efficiency at the nominal current density (~4% i.e. from 79% unmixed to 75% mixed configuration).

The different capability of reducing the H_2 concentration in O_2 for these two configurations appears quite significant at 90 °C suggesting that an increase of temperature may also favour the chemical recombination process (composite catalyst approach) compared to the electrochemical oxidation of hydrogen to protons (unmixed approach).

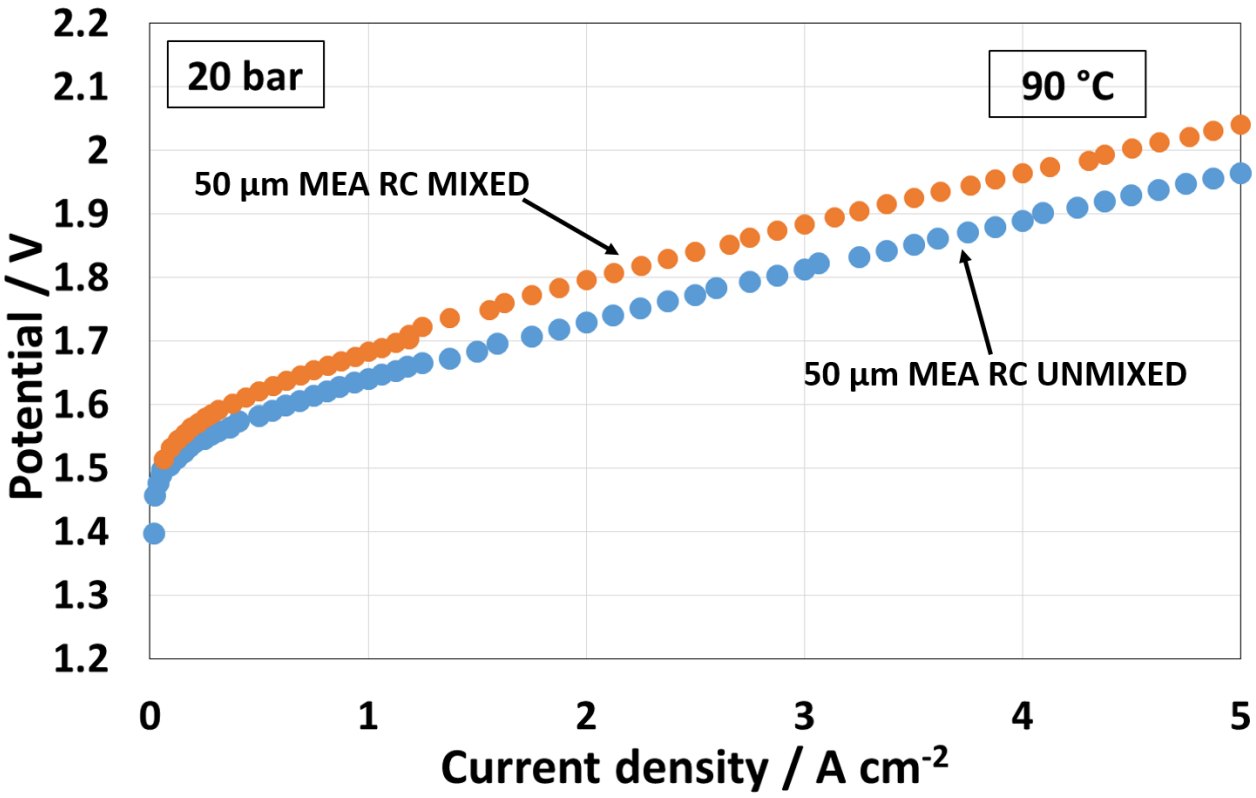

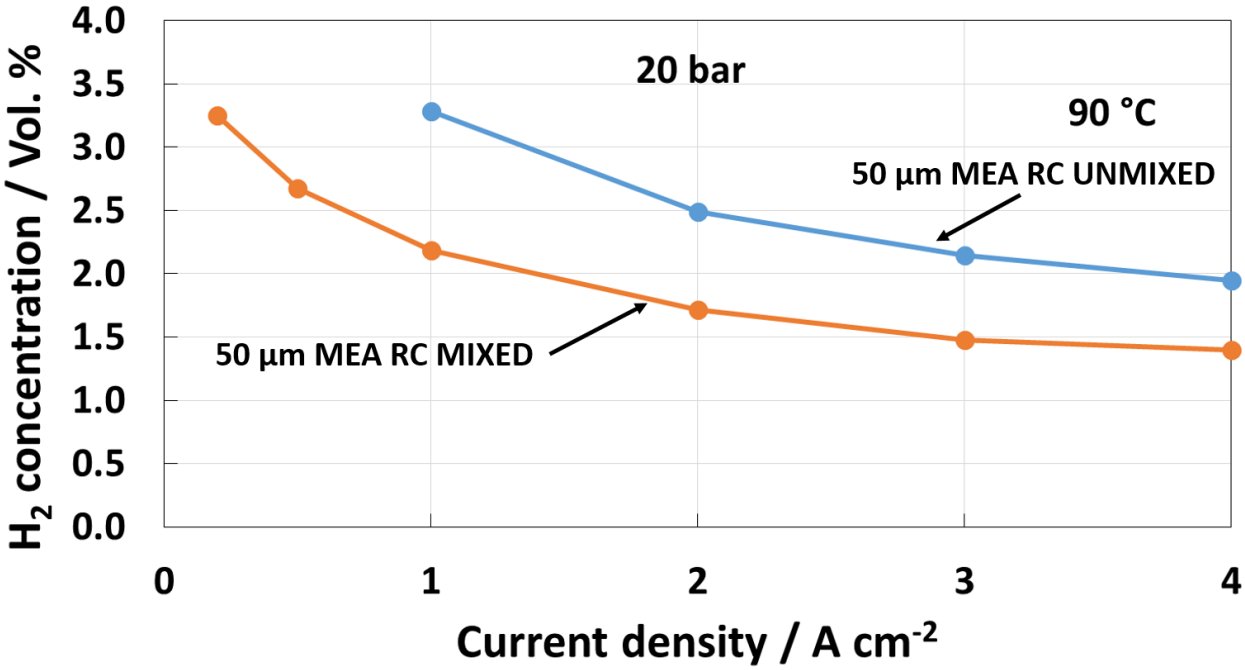

Fig. 7. Polarization curves and H_2 concentration in O_2 for RC MIXED and UNMIXED based MEAs.

0 shows that, at 55 °C, the MEA containing the PtCo catalyst at the anode, even in the mixed configuration, is performing better in terms of voltage efficiency compared to a bare MEA based on the same membrane. Thus, two effects are played by the recombination catalyst i.e. reduction of H_2 concentration in O_2 and slight increase of electrochemical performance. The increase of performance may be in part due to a depolarisation effect (hydrogen oxidation instead of oxygen evolution over the PtCo catalyst) and in part to a contribution to the oxygen evolution. However, the addition of the catalytic recombiner also means a larger loading of precious group metals (0.6 vs. 0.4 mg PGM cm^{-2}_{MEA}). The larger PGM loading in the MEA containing the PtCo catalyst may allow a better current collection for such a thin catalyst layer compared to the bare MEA. However, impedance studies in Fig. 8 do not show relevant change in series resistance. Whereas a variation of the polarisation resistance is clearly observed. A lower polarisation resistance for the PtCo based MEA is effectively observed at 1.5 V but it is even more evident at higher cell voltages (1.8 V) corresponding to higher current density. Under these conditions, the

hydrogen permeation rate is higher and the PtCo catalyst contributes to depolarizing the anode by oxidation of the permeated H_2.

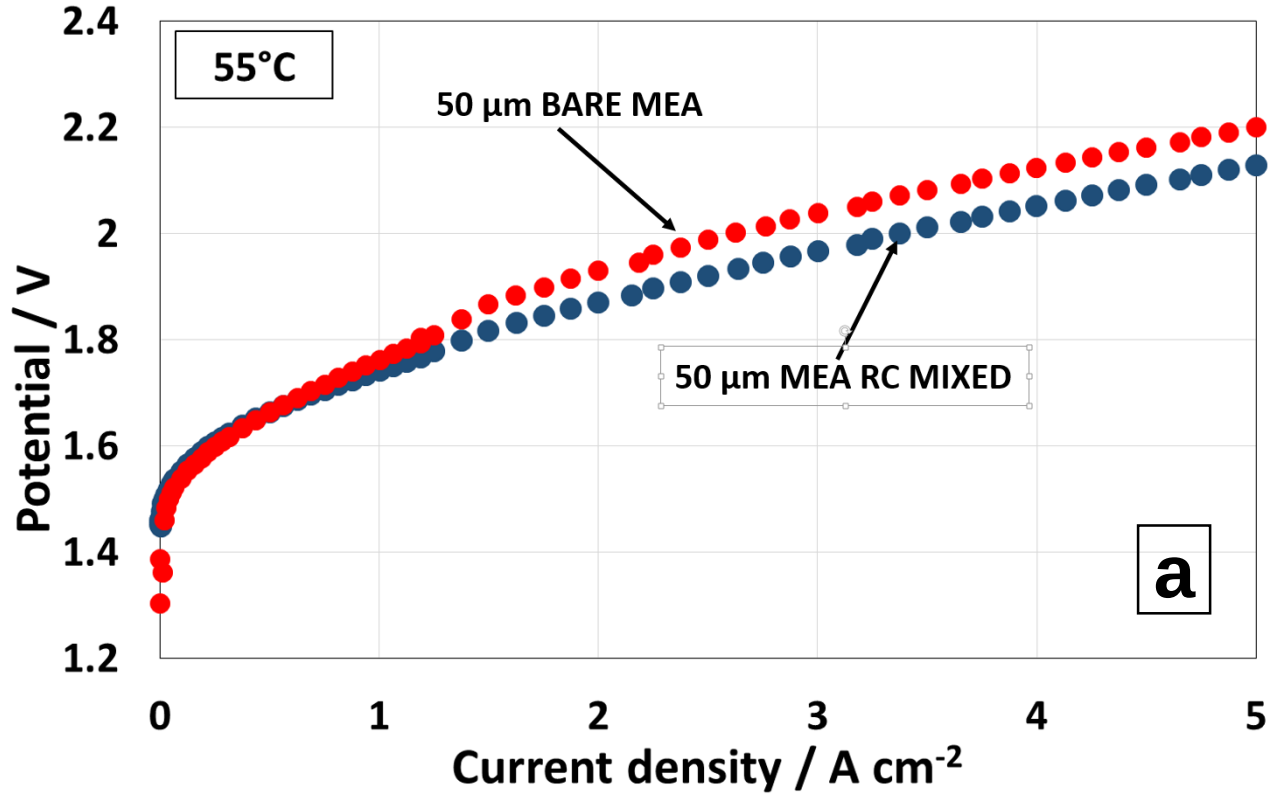

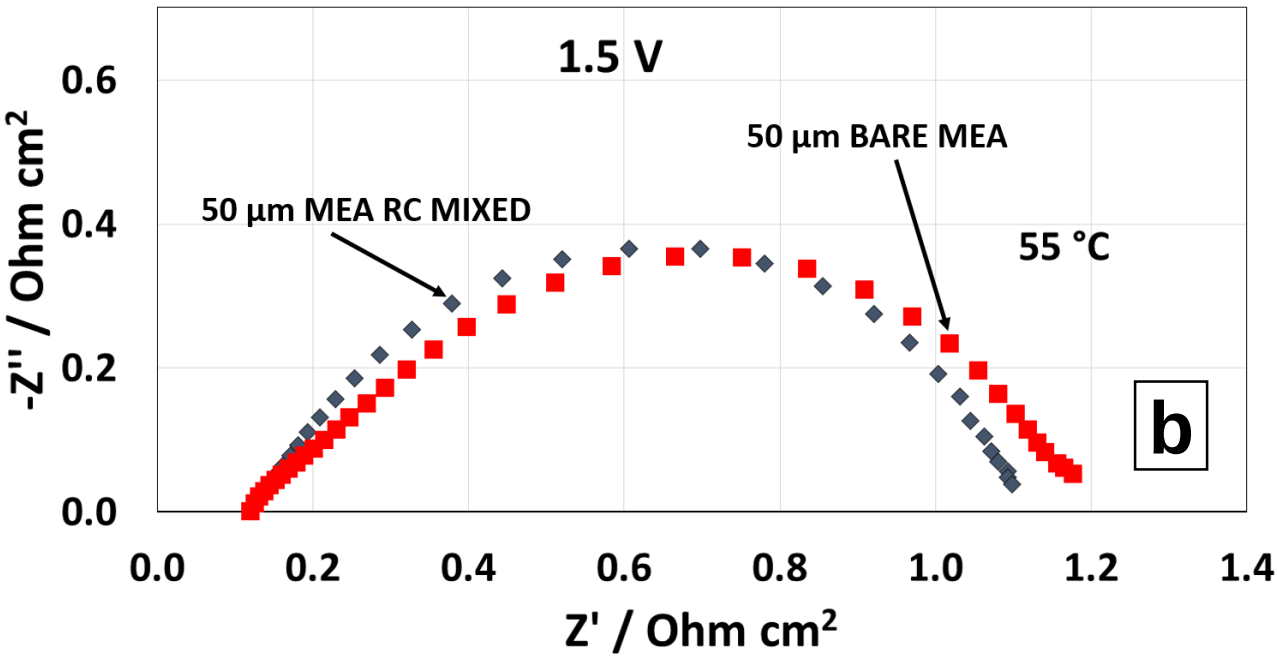

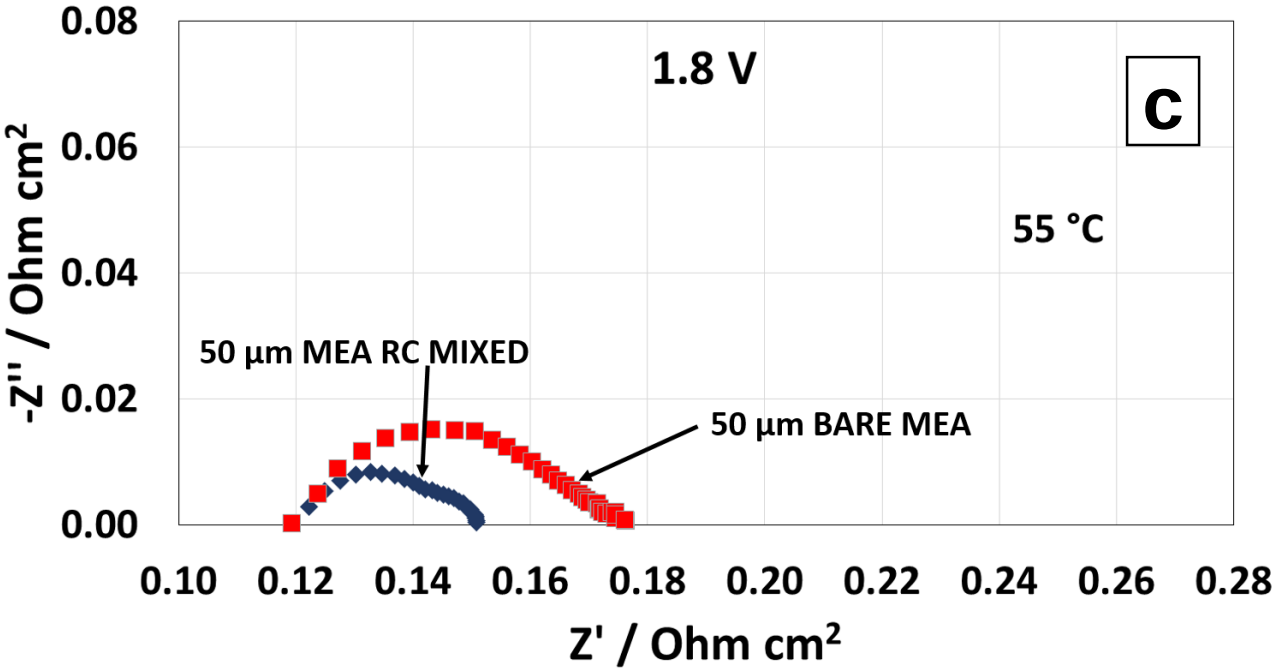

Fig. 8 Polarization curves (a) and impedance spectroscopy at 1.5 V (b) and 1.8 V (c) comparison for bare and RC MIXED configuration based MEAs.

For the same configuration, e.g. mixed catalyst layer, the H_2 concentration was higher at 90° C compared to 55°C (Fig. 9). This behaviour is essentially due to the larger membrane swelling at 90°C causing an increase of gas crossover. An increase of temperature improves the voltage efficiency but it also increases the permeation rate and thus the content of H_2 in the oxygen stream (0).

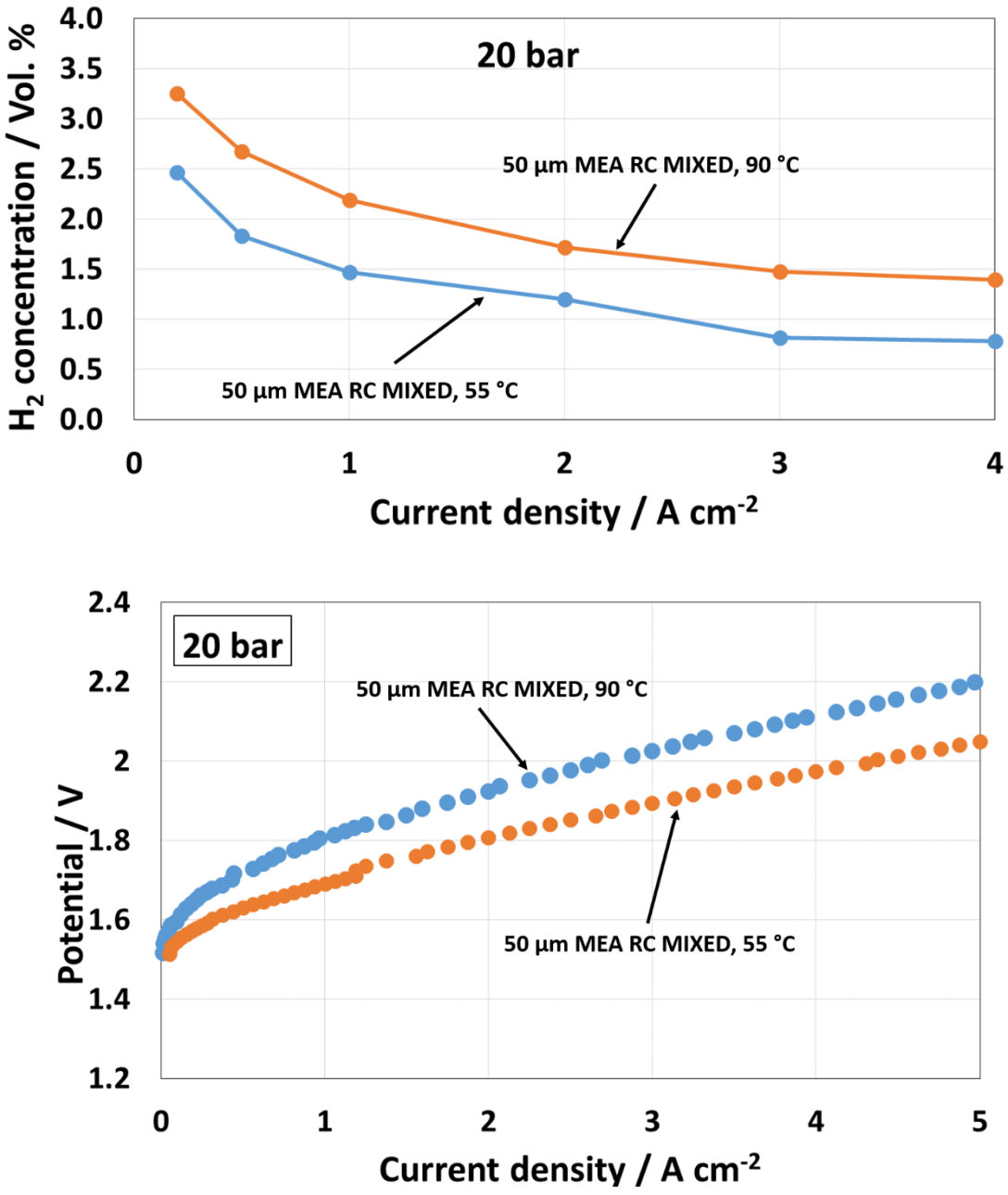

Fig. 9 Polarization curves and H_2 concentration in O_2 comparison at different temperature for the RC MIXED configuration-based MEA.

The Aquivion® membrane is characterised by a high glass transition temperature allowing in principle operation at intermediate temperatures. Operation at 140°C is an interesting trade-off because of the more favourable thermodynamic conditions, enhanced reactions kinetics and lower cooling requirements while avoiding negative effects on the membrane mechanical stability.

However, above 100 °C, the rapid water evaporation from the membrane causes a significant decrease of its proton conduction [1]. Thus, operation at temperatures above 100 °C is only possible if the cell is properly pressurised. In our PEM configuration, being water supplied only to the anode, this compartment needs to be pressurised for operation at temperatures larger than 100 °C. The cathodic layer is kept humidified by the water diffusion through the membrane. This occurs by the effect of the water concentration gradient between anode and cathode. Beside the anode, pressurisation of the cathode also helps in keeping liquid water inside the cell at temperatures above 100 °C. Thus, during PEM electrolysis operation at 140 °C, it was necessary to keep constant the anode compartment pressure at 5.5 bar abs. whereas the cathode pressure was varied as in the experiments carried out at lower temperature.

At 140°C, the electrochemical performance at high current densities, with the cathode kept at ambient pressure, was worse than at higher cathode pressures probably due to the relevant presence of water vapour in the gas phase (Fig. 10). Water permeation from anode to cathode at 140°C produced indeed a quick water vaporization at the cathode kept at ambient pressure causing mass transfer constraints for hydrogen evolution. This is particular evident at high current density and it influences negatively the cell efficiency (Fig. 10) [40]**Error! Reference source not found.**. The trend between 10 and 20 bar was in line with what observed at lower temperatures i.e. the cell voltage was increasing slightly as the pressure was increased according to the Nernst law. In this case, the pressurization of the cathode allowed to keep the permeated water in a liquid form favouring hydrogen gas separation from the liquid phase. Impedance spectra were carried out at 1.5 V only, because at 1.8 V, the electrical current at 140 °C exceeded the limit of the ac-impedance analysis booster. However, also impedance spectroscopy confirmed this peculiar trend at intermediate currents. Polarisation resistance decreased by

decreasing the cathode pressure from 20 to 10 bar and increased again at ambient cathode pressure.

At very low current density and at ambient cathode pressure, the presence of water vapour did not hinder much the hydrogen evolution because of the small production rate. It is noted that at 140 °C, under pressurised conditions, e.g. 20 bar cathode, 5.5 bar anode, at 5 A cm^{-2}, the cell voltage was as low as 1.8 V. This represents a significant gain in cell performance showing the importance of operation at intermediate temperatures.

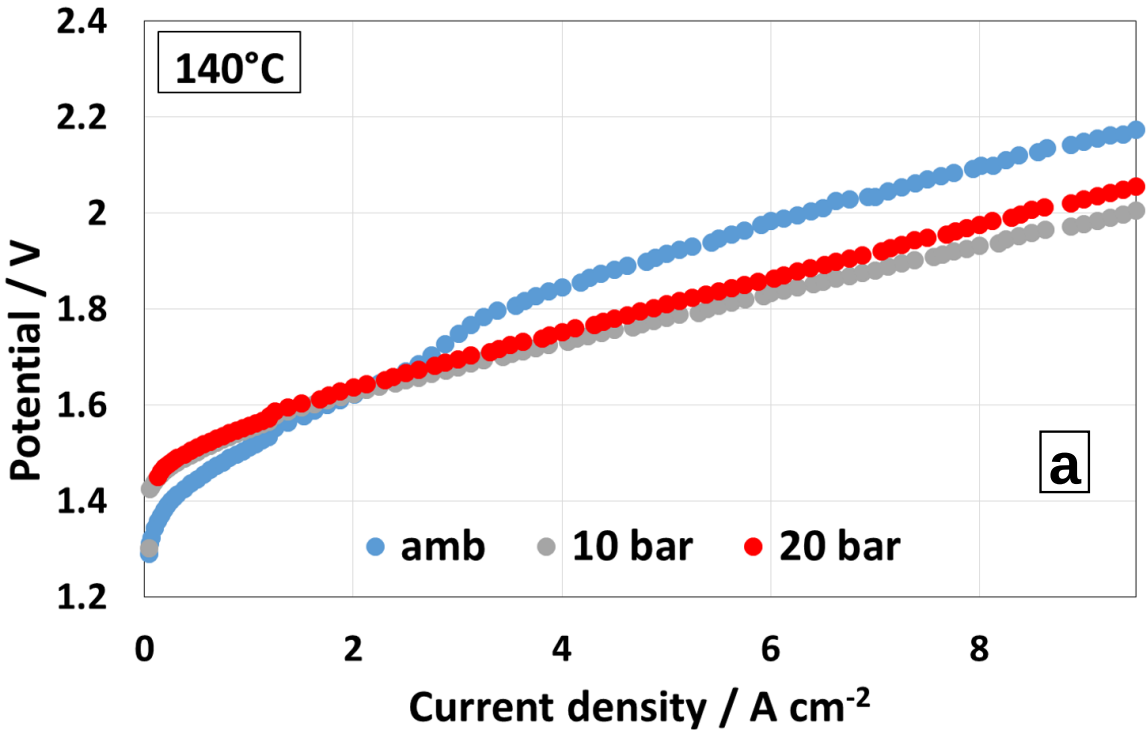

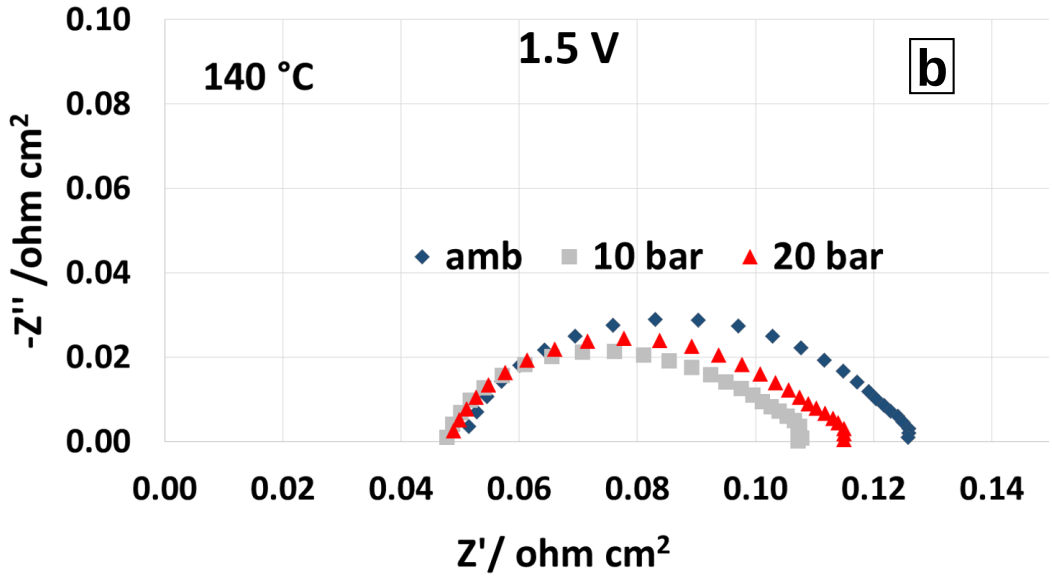

Fig. 10 Polarization curves (a) and impedance spectroscopy (b) comparison at 140°C and different cathodic pressures for RC MIXED MEA. The anode pressure was kept constant at 5.5 bar.

It is now useful to analyse the effect of the operating cell temperature on the hydrogen concentration in the oxygen stream. Figure 11 shows the tests carried out from 55°C to 140°C under the conditions discussed above (ambient pressure is used at the anode until 90 °C and it is increased to 5.5 bar abs at 140 °C). An increase of temperature caused an increase of the H_2 concentration in O_2 when passing from 55°C to 90°C. However, a different behaviour was observed at 140°C. The H_2 crossover under differential pressure operation (with the cathode kept at higher pressure than the anode) was relatively constant from low to high current density. It is important to consider that the anode pressurisation promotes the recombination process over the recombination catalyst surface.

However, this trend was not observed when the cathode was kept at ambient pressure. An unusual increase of hydrogen concentration with the current density was observed. Of course, this appears associated to the increase of the hydrogen permeation rate with the

increase of current density but the usual prevailing counteracting effect of the hydrogen dilution caused by the increased oxygen evolution was less relevant in this situation.

In principle, this trend was in part caused by the very efficient behaviour of the recombination catalyst in the presence of pressurised oxygen (5.5 bar) at 140 °C especially at low current density and ambient cathode pressure when the hydrogen permeation rate was relatively low. Under these conditions, the evolved H_2 gas needs competing with water vapour (ambient cathode pressure) to permeate to the anode. The pressurised oxygen at the anode produces a differential pressure with an opposite direction acting as physical barrier. All these phenomena were probably impeding relevant amounts of hydrogen to permeate to the anode at low current density and the few permeated molecules were also efficiently oxidised by the recombination catalyst. Upon increasing the current density to certain values, the hydrogen permeation increased significantly because of the supersaturation of the cathode catalytic layer causing the observed increase of H_2 concentration in O_2. Thus, this trend is essentially determined by a trade-off between the increased hydrogen permeation rate, caused by the increase in current density, and the counteracting activity of the recombination catalyst at high temperature that is especially high in the presence of low H_2 permeation values.

When the cathode was also pressurised at 140 °C, an increased H_2 permeation occurred already at low current densities by the pressure effect. Under these conditions, the larger H_2 permeation was less counteracted by the activity of the recombination catalyst even if this was still promoted by the presence of a small oxygen pressure at the anode. Upon pressurisation of the cathode at 140°C, the relevant effects were an increased hydrogen permeation rate, the dilution of the permeated hydrogen by the evolved oxygen, the still relevant activity of the recombination catalyst and the transport of liquid water to the cathode (electroosmotic drag) associated to the increase of current density. These

phenomena possibly compensated each other and the H_2 concentration in O_2 remained almost constant with the current density. Moreover, the higher catalyst activity observed at 140 °C in comparison to lower temperatures has a positive effect on reducing the H_2 concentration by balancing the negative effects of membrane swelling.

Regarding the effect of the cathode pressure, a usual trend was observed at 55°C with the concentration of H_2 in the anodic stream decreasing as a function of the increase of current density and decrease of pressure (Fig. 11 a). At 90°C (Fig. 11 b), the enhanced activity of the recombination catalyst caused a change of this trend especially at low current densities and low cathodic pressures when the H_2 permeation rate was low. At 90°C and ambient pressure, the H_2 concentration in O_2 was very low at low current density and increased with the increase of H_2 production rate. This phenomenon was relatively similar to that occurring at 140°C and already commented. At 140 °C this was more evident where the activity of the recombination catalyst was further enhanced by the temperature and mild anode pressurization, as required to avoid water boiling (Fig. 11 c).

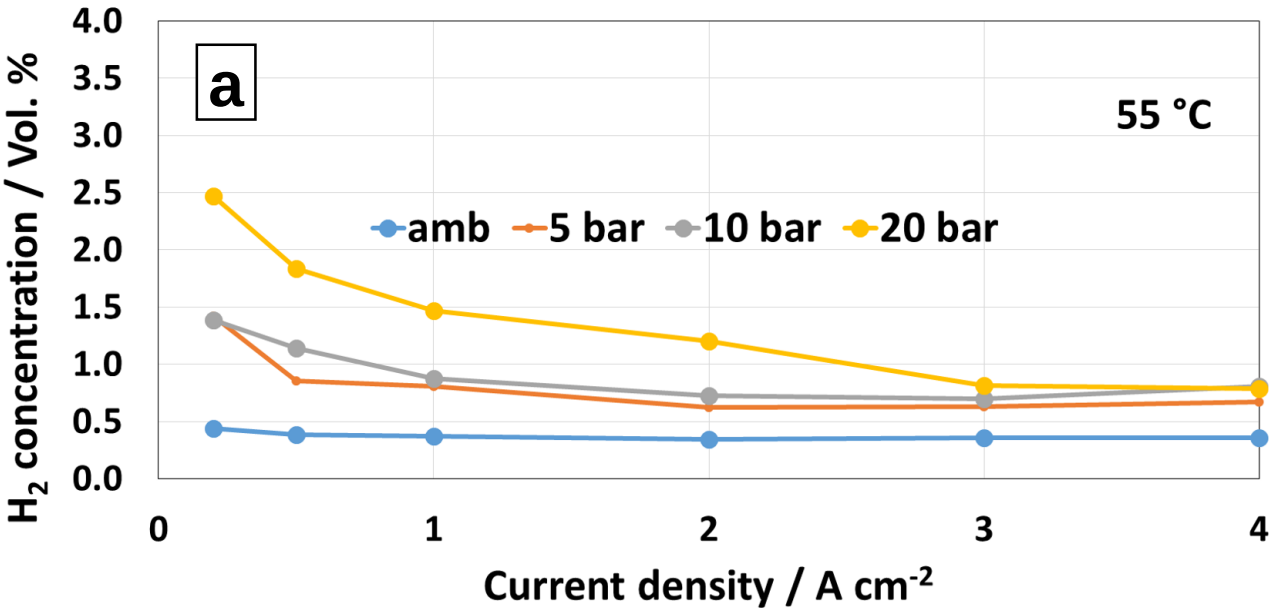

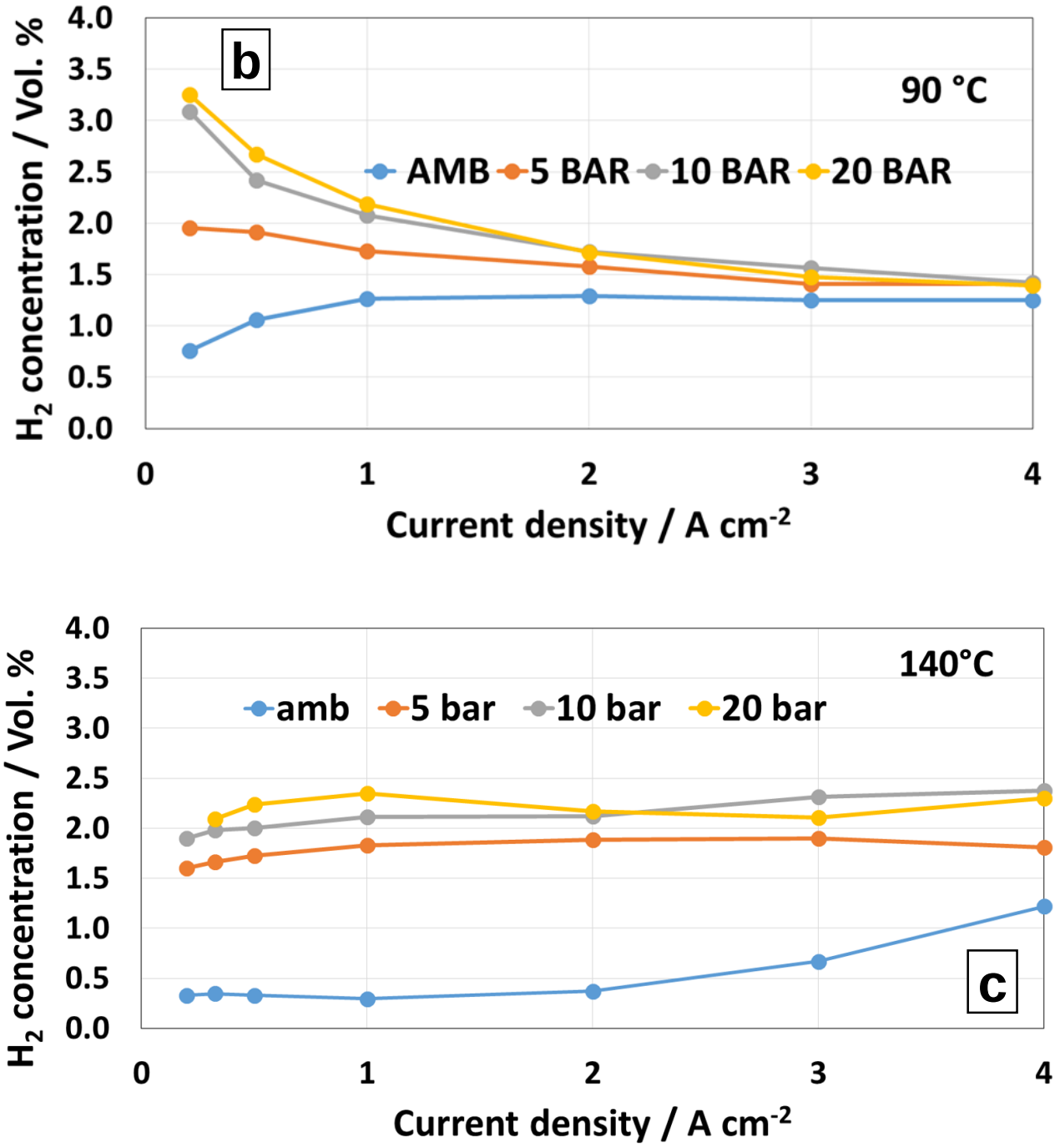

Fig. 11 Comparison of the H_2 concentration in O_2 at different temperatures and pressures for MIXED RC based MEA. Ambient anode pressure was used at 55 °C and 90 °C whereas a pressure of 5.5 bar was used at 140°C.

The effect of pressure on the electrochemical performances of the MEA containing the recombination catalyst in a mixed configuration at 55°C is shown in 0. Under these specific operative conditions, a pressure increase from 0 to 10-20 bar caused an increase of cell voltage as expected from the Nernst equation. This is more evident in the impedance

spectra where an increase of polarization resistance with pressure is observed at two different potentials 1.5 V and 1.8 V.

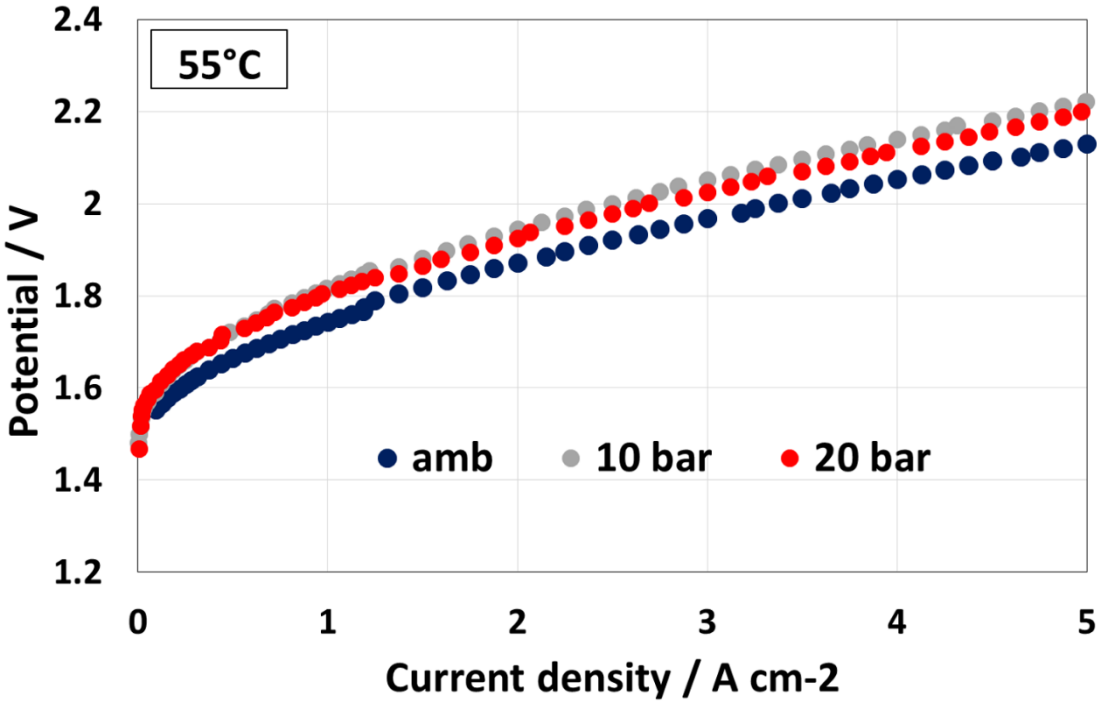

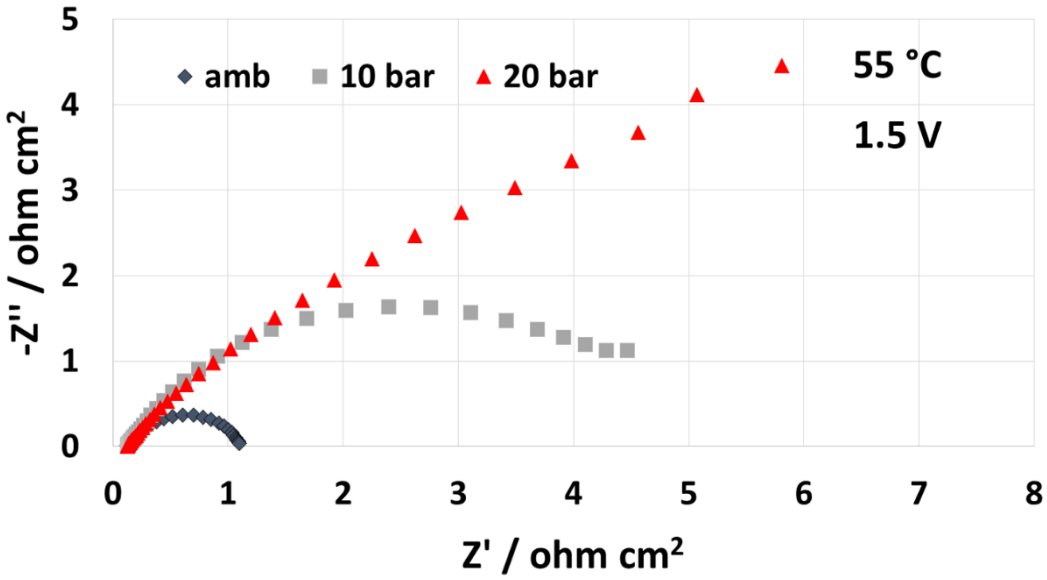

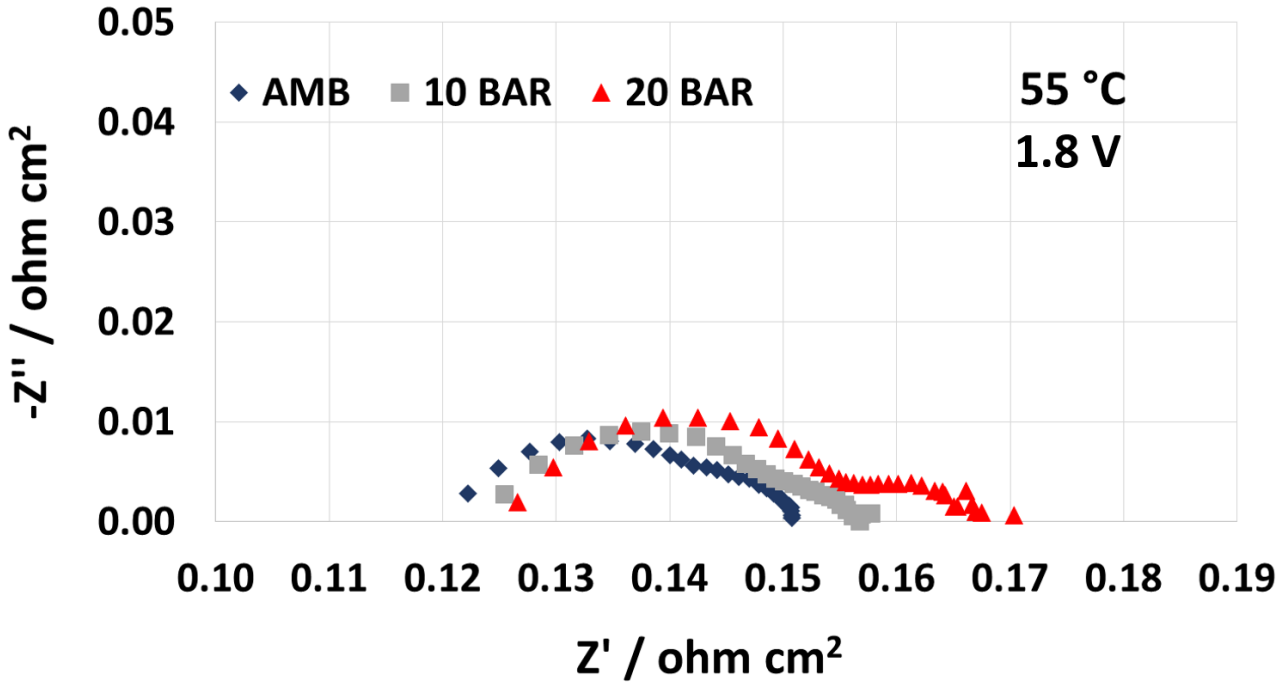

Fig. 12 Comparison of polarization curves and impedance spectra at 55°C and different pressure for RC-based mixed MEA.

The effect of the cathodic pressure was smaller at 90°C with similar electrochemical performances in the analysed pressure range (**Error! Reference source not found.**) [40]. The impedance spectra still showed larger polarization resistance with the increase of pressure at 90°C according to the Nernst law. This was more evident at 1.5 V where the shift in the Nernst potential had a larger impact on the polarization resistance. Such features were amplified by the impedance spectroscopy analysis whereas with minimal effects were observed in the polarization curves. In general, the increase of pressure has a modest effect on the electrolyser voltage efficiency whereas it allows reducing significantly the energy consumption of the downstream mechanical gas compression especially in refuelling stations applications. It appears that a further increase of the operating differential pressure in PEM electrolysis, in the presence of thin membranes, can be sustained by a proper development of the integrated recombination catalyst technology.

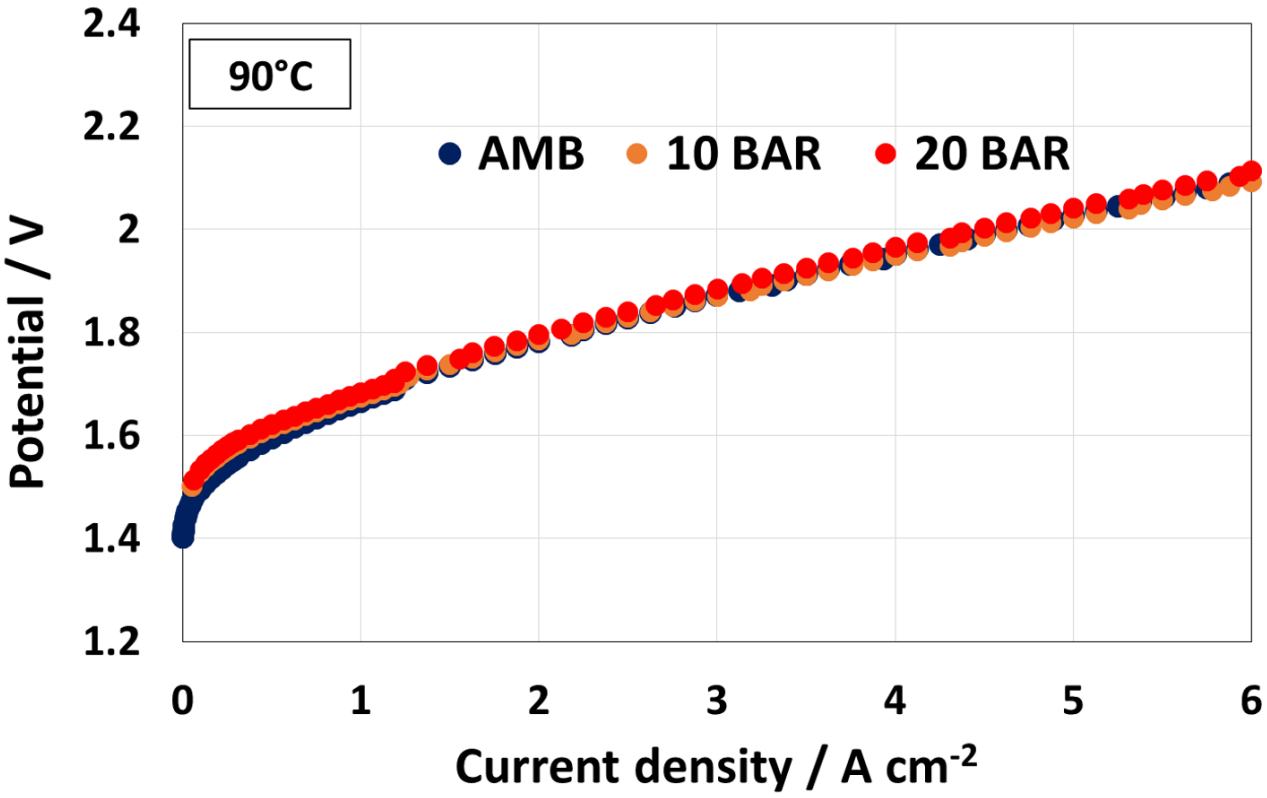
90°C
AMB
10 BAR
20 BAR
Potential / V
2.4
2.2
2
1.8
1.6
1.4
1.2
0
1
2
3
4
5
6
Current density / A cm-2

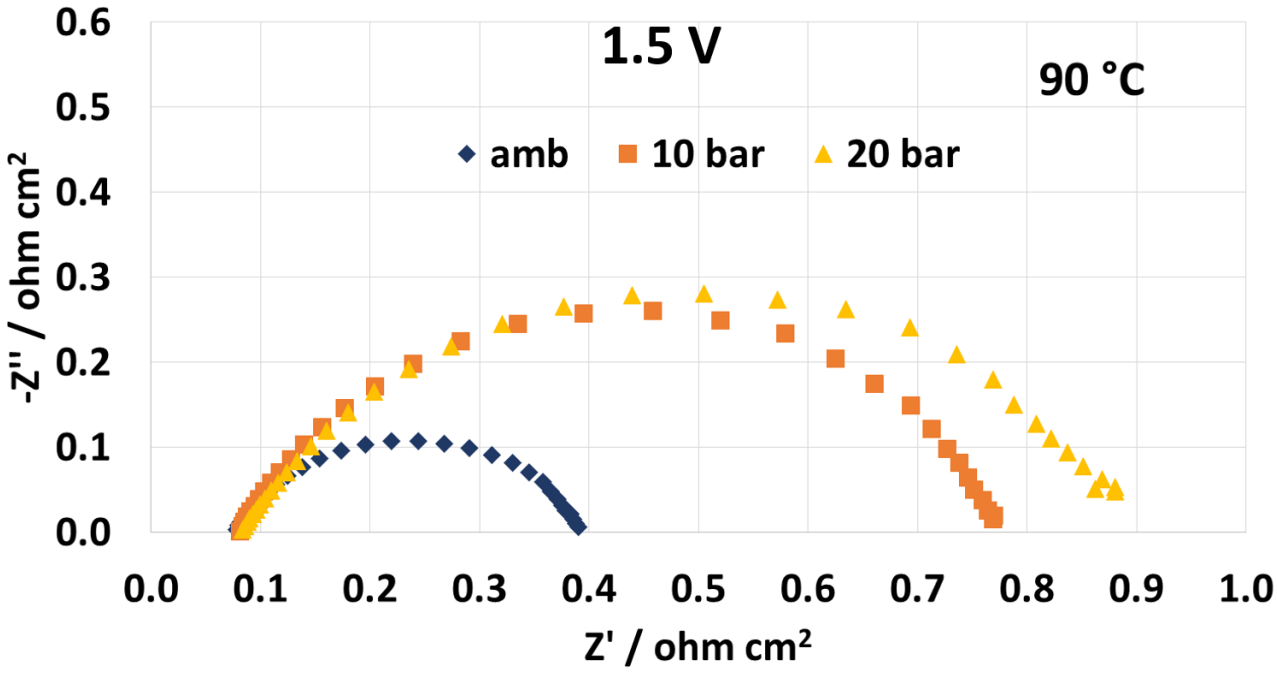
1.5 V
90 °C
amb
10 bar
20 bar
-Z'' / ohm cm²
0.6
0.5
0.4
0.3
0.2
0.1
0.0
0.0
0.1
0.2
0.3
0.4
0.5
0.6
0.7
0.8
0.9
1.0
Z' / ohm cm²

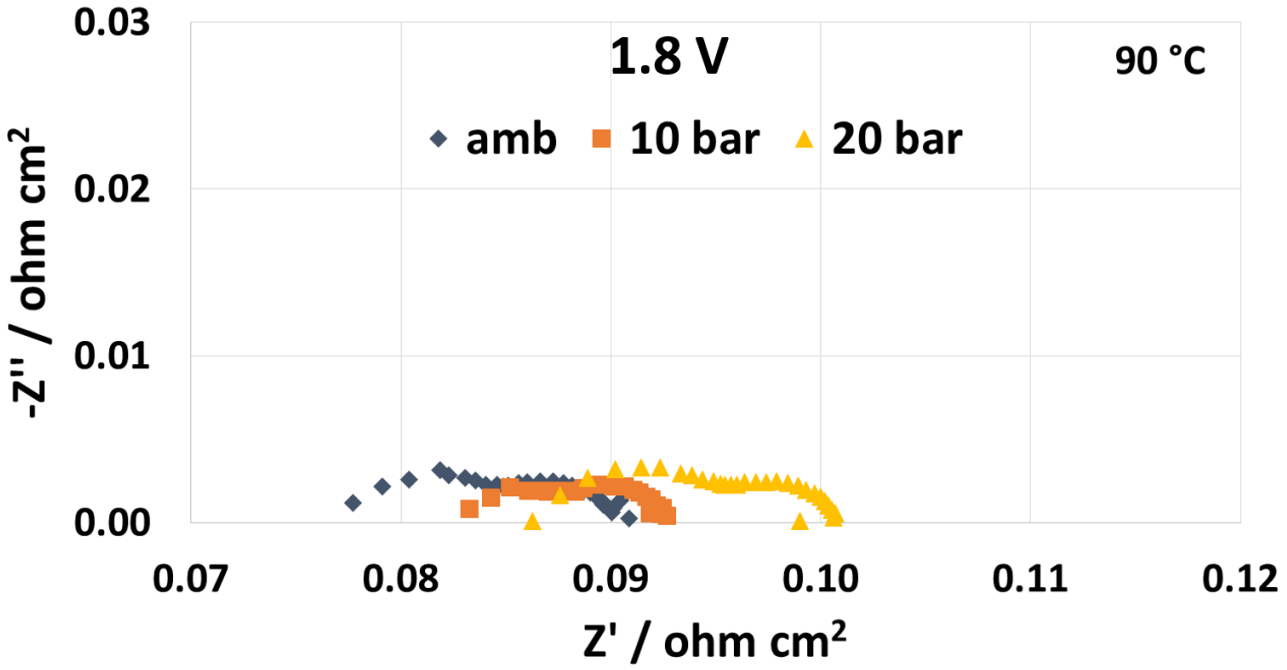

Fig. 13 Comparison of polarization curves and impedance spectra at 90°C and different pressure for RC-based mixed MEA.

4. Conclusions

A PtCo alloy recombination catalyst was integrated in a membrane-electrode assembly and investigated for reducing the H_2 concentration in the oxygen stream during PEM electrolysis operation in the presence of a thin 50 µm PFSA Aquivion® membrane. The PtCo catalyst properties were optimised to provide enhanced activity through tailoring the catalytic recombiner surface chemistry, electronic effects and mean crystallite size.

Two different MEA configurations were studied. A dual-layer (unmixed) anode configuration where the PtCo alloy catalyst was integrated in the membrane-electrode assembly between the membrane and the IrRuOx anode catalyst and a mixed layer (composite anode layer) configuration made of a mixture of PtCo and IrRuOx. Both configurations showed good performance for the oxidation of the permeated hydrogen allowing to achieve enhanced safety characteristics under differential pressure. The mixed

configuration showed better activity for reducing the hydrogen concentration at the anode but slightly lower electrochemical performance. Two mechanisms were hypothesized: one mainly consisting in an electrochemical oxidation of the permeated H_2 to protons (unmixed configuration) and the other consisting in a direct chemical recombination mechanism (mixed configuration) of the permeated hydrogen and evolved oxygen into water. The performance of the MEAs containing the recombination catalyst was better than a bare MEA while producing a decrease of the H_2 content at the anode. This allowed extending the load range under differential pressure. The effects of the cathodic pressure and cell temperature on the electrochemical performance and H_2 content at the anode were investigated. At 55°C and 20 bar differential pressure, in the presence of the PtCo catalytic recombiner and a thin 50 µm PFSA membrane, the hydrogen concentration in the anodic oxygen stream was well below the flammability limit at a current density as low as 0.2 A cm^{-2}. This corresponds to about 5% partial load operation for a nominal operating current density of 4 A cm^{-2} corresponding to about 70 % voltage efficiency at 55°C. An enhancement of the dynamic characteristics for PEM electrolysis is expected compared to conventional systems (minimum load range of 20%).

The mixed configuration was also investigated at an intermediate operating temperature of 140 °C at different cathodic pressures using a slightly pressurised anode. An excellent performance of 4 A cm^{-2} at 1.75 V at 140 °C, 20 bar cathode pressure and 5.5 bar anode pressure was recorded. This performance was achieved in the presence of a H_2 concentration in the oxygen stream of about 2 % that was almost constant through the overall current density range. Such results indicate good perspectives for intermediate temperature PEM electrolysis operation using thin membranes in order to increase electrochemical efficiency, reduce energy consumption for cooling and make better use of the higher quality heat released under electrolysis operation at high current density.

Acknowledgements

CNR-ITAE authors acknowledge the financial support from the NEPTUNE project. This project has received funding from Fuel Cells and Hydrogen 2 Joint Undertaking under grant agreement N 779540. This Joint Undertaking receives support from the European Union's Horizon 2020 research and innovation programme and Hydrogen Europe and Hydrogen Europe Research. The authors also thank Solvay Specialty Polymers for supplying the membrane and the ionomer, ITM Power (UK) for supplying the high-pressure single cell test fixture.

References

[1] A.S. Aricò, S. Siracusano, N. Briguglio, V. Baglio, A. Di Blasi, V. Antonucci, Polymer electrolyte membrane water electrolysis: Status of technologies and potential applications in combination with renewable power sources, J. Appl. Electrochem. 43 (2013) 107–118. https://doi.org/10.1007/s10800-012-0490-5.

[2] M.T. Dinh Nguyen, A. Ranjbari, L. Catala, F. Brisset, P. Millet, A. Aukauloo, Implementing molecular catalysts for hydrogen production in proton exchange membrane water electrolysers, Coord. Chem. Rev. 256 (2012) 2435–2444. https://doi.org/10.1016/j.ccr.2012.04.040.

[3] M. Carmo, D.L. Fritz, J. Mergel, D. Stolten, A comprehensive review on PEM water electrolysis, Int. J. Hydrogen Energy. 38 (2013) 4901–4934. https://doi.org/10.1016/j.ijhydene.2013.01.151.

[4] H. Dagdougui, C. Bersani, R. Sacile, , A. Ouammi "Hydrogen Infrastructure for Energy Applications: Production, Storage, Distribution and Safety", Chapter 4 - Hydrogen Storage and Distribution: Implementation Scenarios, Section 3.1: Compressed Gaseous Hydrogen, Elsevier Inc. ISBN 978-0-12-812036-1; DOI https://doi.org/10.1016/C2016-0-03214-X.

[5] N. Briguglio, G. Brunaccini, S. Siracusano, N. Randazzo, G. Dispenza, M. Ferraro, R. Ornelas, A.S. Aricò, V. Antonucci, Design and testing of a compact PEM electrolyzer system, Int. J. Hydrogen Energy. 38 (2013) 11519–11529. https://doi.org/10.1016/j.ijhydene.2013.04.091.

[6] D. Saebea, Y. Patcharavorachot, V. Hacker, S. Assabumrungrat, A. Arpornwichanop, S. Authayanun, Analysis of unbalanced pressure PEM electrolyzer for high pressure hydrogen production, Chem. Eng. Trans. 57 (2017) 1615–1620.

https://doi.org/10.3303/CET1757270.

[7] G. Chisholm, L. Cronin, M.D. Symes, Decoupled electrolysis using a silicotungstic acid electron-coupled-proton buffer in a proton exchange membrane cell, Electrochim. Acta. 331 (2020). https://doi.org/10.1016/j.electacta.2019.135255.

[8] C. Immerz, M. Schweins, P. Trinke, B. Bensmann, M. Paidar, T. Bystroň, K. Bouzek, R. Hanke-Rauschenbach, Experimental characterization of inhomogeneity in current density and temperature distribution along a single-channel PEM water electrolysis cell, Electrochim. Acta. 260 (2018) 582–588. https://doi.org/10.1016/j.electacta.2017.12.087.

[9] A.C. Olesen, S.H. Frensch, S.K. Kær, Towards uniformly distributed heat, mass and charge: A flow field design study for high pressure and high current density operation of PEM electrolysis cells, Electrochim. Acta. 293 (2019) 476–495. https://doi.org/10.1016/j.electacta.2018.10.008.

[10] S.H. Frensch, A.C. Olesen, S.S. Araya, S.K. Kær, Model-supported characterization of a PEM water electrolysis cell for the effect of compression, Electrochim. Acta. 263 (2018) 228–236. https://doi.org/10.1016/j.electacta.2018.01.040.

[11] S. Siracusano, S. Trocino, N. Briguglio, V. Baglio, A.S. Aricò, Electrochemical impedance spectroscopy as a diagnostic tool in polymer electrolyte membrane electrolysis, Materials (Basel). 11 (2018). https://doi.org/10.3390/ma11081368.

[12] G. Tsotridis, A. Pilenga in "EU harmonised terminology for low temperature water electrolysis for energy storage applications", Publications Office of the European Union Publisher, ISBN: 978-92-79-90387-8 (online), 978-92-79-90388-5 (print).

[13] S.A. Grigoriev, V.I. Porembskiy, S.V. Korobtsev, V.N. Fateev, F. Auprêtre, P. Millet, High-pressure PEM water electrolysis and corresponding safety issues, Int. J.

Hydrogen Energy. 36 (2011) 2721–2728. https://doi.org/10.1016/j.ijhydene.2010.03.058.

[14] G. Papakonstantinou, K. Sundmacher, H_2 permeation through N117 and its consumption by IrOx in PEM water electrolyzers, Electrochem. Commun. 108 (2019). https://doi.org/10.1016/j.elecom.2019.106578.

[15] H. Ito, T. Maeda, A. Nakano, H. Takenaka, Properties of Nafion membranes under PEM water electrolysis conditions, Int. J. Hydrogen Energy. 36 (2011) 10527–10540. https://doi.org/10.1016/J.IJHYDENE.2011.05.127.

[16] P. Trinke, B. Bensmann, S. Reichstein, R. Hanke-Rauschenbach, K. Sundmacher, Hydrogen permeation in PEM electrolyzer cells operated at asymmetric pressure conditions, J. Electrochem. Soc. 163 (2016) F3164–F3170. https://doi.org/10.1149/2.0221611jes.

[17] P. Trinke, P. Haug, J. Brauns, B. Bensmann, R. Hanke-Rauschenbach, T. Turek, Hydrogen crossover in PEM and alkalinewater electrolysis: Mechanisms, direct comparison and mitigation strategies, J. Electrochem. Soc. 165 (2018) F502–F513. https://doi.org/10.1149/2.0541807jes.

[18] A. Skulimowska, M. Dupont, M. Zaton, S. Sunde, L. Merlo, D.J. Jones, J. Rozière, Proton exchange membrane water electrolysis with short-side-chain Aquivion® membrane and IrO2 anode catalyst, Int. J. Hydrogen Energy. 39 (2014) 6307–6316. https://doi.org/10.1016/j.ijhydene.2014.02.082.

[19] D. Bessarabov, P. Millet in "Gas Permeation in PEM Water Electrolyzers", PEM Water Electrolysis, Volume 1, 1st Edition, Series Editors: Bruno Pollet; Elsevier. ISBN: 9780128111451;

[20] F. Marangio, M. Pagani, M. Santarelli, M. Calì, Concept of a high pressure PEM

electrolyser prototype, Int. J. Hydrogen Energy. 36 (2011) 7807–7815. https://doi.org/10.1016/j.ijhydene.2011.01.091.

[21] A.A. Kalinnikov, S.A. Grigoriev, D.G. Bessarabov, Nonequilibrium poroelectroelastic theory for polymer electrolytes under conditions of water electrolysis, Int. J. Hydrogen Energy. 44 (16) (2019), 7889-7904. https://doi.org/10.1016/j.ijhydene.2019.02.025.

[22] D. Bessarabov, Membranes with recombination catalyst for hydrogen crossover reduction: Water electrolysis, in: ECS Trans., 2018: pp. 17–25. https://doi.org/10.1149/08511.0017ecst.

[23] S.A. Grigoriev, P. Millet, S.V. Korobtsev, V.I. Porembskiy, M. Pepic, C. Etievant, C. Puyenchet, V.N. Fateev, Hydrogen safety aspects related to high-pressure polymer electrolyte membrane water electrolysis, Int. J. Hydrogen Energy. 34 (2009) 5986–5991. https://doi.org/10.1016/J.IJHYDENE.2009.01.047.

[24] V. Schröder, B. Emonts, H. Janßen, H.-P. Schulze, Explosion limits of hydrogen/oxygen mixtures at initial pressures up to 200 bar, Chem. Eng. Technol. 27 (2004) 847–851. https://doi.org/10.1002/ceat.200403174.

[25] R. Owston, V. Magi, J. Abraham, Interactions of hydrogen flames with walls: Influence of wall temperature, pressure, equivalence ratio, and diluents, Int. J. Hydrogen Energy. 32 (2007) 2094–2104. https://doi.org/10.1016/J.IJHYDENE.2006.07.030.

[26] H.A. Gasteiger, S.S. Kocha, B. Sompalli, F.T. Wagner, Activity benchmarks and requirements for Pt, Pt-alloy, and non-Pt oxygen reduction catalysts for PEMFCs, Appl. Catal. B Environ. 56 (2005) 9–35. https://doi.org/10.1016/J.APCATB.2004.06.021.

[27] P. Trinke, B. Bensmann, R. Hanke-Rauschenbach, Current density effect on hydrogen permeation in PEM water electrolyzers, Int. J. Hydrogen Energy. 42 (2017) 14355–14366. https://doi.org/10.1016/j.ijhydene.2017.03.231.

[28] M. Schalenbach, M. Carmo, D.L. Fritz, J. Mergel, D. Stolten, Pressurized PEM water electrolysis: Efficiency and gas crossover, Int. J. Hydrogen Energy. 38 (2013) 14921–14933. https://doi.org/10.1016/J.IJHYDENE.2013.09.013.

[29] M. Inaba, T. Kinumoto, M. Kiriake, R. Umebayashi, A. Tasaka, Z. Ogumi, Gas crossover and membrane degradation in polymer electrolyte fuel cells, Electrochim. Acta. 51 (2006) 5746–5753. https://doi.org/10.1016/j.electacta.2006.03.008.

[30] G. Papakonstantinou, K. Sundmacher, H2 permeation through N117 and its consumption by IrOx in PEM water electrolyzers, Electrochem. Commun. 108 (2019). https://doi.org/10.1016/j.elecom.2019.106578.

[31] J. Zhang, H. Zhang, J. Wu, J. Zhang, Hydrogen Crossover, in: Pem Fuel Cell Test. Diagnosis, Elsevier, 2013: pp. 171–185. https://doi.org/10.1016/b978-0-444-53688-4.00006-1.

[32] V. Shepelin, D. Koshmanov, E. Chepelin, Catalyst for recombination of hydrogen and oxygen in confined spaces under high concentrations of hydrogen, Nucl. Technol. 178 (2012) 29–38. https://doi.org/10.13182/NT12-A13545.

[33] Math hydrogen catalytic recombiner: Engineering model for dynamic full-scale calculations, A.V. Avdeenkova, Vl.V. Sergeev, A.V. Stepanov, A.A. Malakhov, D.Y. Koshmanov, S.L. Soloviev, D.G. Bessarabov, Int. J. Hydrogen Energy, 43 (52), (2018) 23523-23537.

[34] M. Watanabe, H. Uchida, M. Emori, Analyses of self-humidification and suppression of gas crossover in Pt-dispersed polymer electrolyte membranes for fuel cells, J.

Electrochem. Soc. 145 (1998) 1137–1141. https://doi.org/10.1149/1.1838429.

[35] D. Bessarabov, A.J. Kruger, S.M. Luopa, J. Park, A.A. Molnar, K.A. Lewinski, Gas crossover mitigation in PEM water electrolysis: Hydrogen cross-over benchmark study of 3M's Ir-NSTF based electrolysis catalyst-coated membranes, in: ECS Trans., 2016: pp. 1165–1173. https://doi.org/10.1149/07514.1165ecst.

[36] S. Giancola, M. Zatoń, Á. Reyes-Carmona, M. Dupont, A. Donnadio, S. Cavaliere, J. Rozière, D.J. Jones, Composite short side chain PFSA membranes for PEM water electrolysis, J. Memb. Sci. 570–571 (2019) 69–76. https://doi.org/10.1016/j.memsci.2018.09.063.

[37] M. Schalenbach, D. Stolten, High-pressure water electrolysis: Electrochemical mitigation of product gas crossover, Electrochim. Acta. 156 (2015) 321–327. https://doi.org/10.1016/J.ELECTACTA.2015.01.010.

[38] C. Klose, P. Trinke, T. Böhm, B. Bensmann, S. Vierrath, R. Hanke-Rauschenbach, S. Thiele, Membrane interlayer with PT recombination particles for reduction of the anodic hydrogen content in PEM water electrolysis, J. Electrochem. Soc. 165 (2018) F1271–F1277. https://doi.org/10.1149/2.1241814jes.

[39] T. Bystron, M. Paidar, T. Klicpera, M. Schuster K. Bouzek in "Proton Exchange Membrane Water Electrolysers: Materials, Construction and Performance" Chapter 3 Pages 59 - 93 in "Electrochemical Methods for Hydrogen Production", Editor: Keith Scott, RSC Publishing, book series: Energy and Environment Series, https://doi.org/10.1039/9781788016049.]

[40] N. Briguglio, S. Siracusano, G. Bonura, D. Sebastián, A.S. Aricò, Flammability reduction in a pressurised water electrolyser based on a thin polymer electrolyte membrane through a Pt-alloy catalytic approach, Appl. Catal. B Environ. 246 (2019)

254–265. https://doi.org/10.1016/j.apcatb.2018.12.079.

[41] S. Siracusano, C. Oldani, M.A. Navarra, S. Tonella, L. Mazzapioda, N. Briguglio, A.S. Aricò, Chemically stabilised extruded and recast short side chain Aquivion® proton exchange membranes for high current density operation in water electrolysis, J. Memb. Sci. 578 (2019) 136–148. https://doi.org/10.1016/j.memsci.2019.02.021.

[42] S. Siracusano, V. Baglio, E. Moukheiber, L. Merlo, A.S. Aricò, Performance of a PEM water electrolyser combining an IrRu-oxide anode electrocatalyst and a short-side chain Aquivion membrane, Int. J. Hydrogen Energy. 40 (2015) 14430–14435. https://doi.org/10.1016/J.IJHYDENE.2015.04.159.

[43] B.-S. Lee, S.H. Ahn, H.-Y. Park, I. Choi, S.J. Yoo, H.-J. Kim, D. Henkensmeier, J.Y. Kim, S. Park, S.W. Nam, K.-Y. Lee, J.H. Jang, Development of electrodeposited IrO2 electrodes as anodes in polymer electrolyte membrane water electrolysis, Appl. Catal. B Environ. 179 (2015) 285–291. https://doi.org/10.1016/J.APCATB.2015.05.027.

[44] H. Yu, N. Danilovic, Y. Wang, W. Willis, A. Poozhikunnath, L. Bonville, C. Capuano, K. Ayers, R. Maric, Nano-size IrOx catalyst of high activity and stability in PEM water electrolyzer with ultra-low iridium loading, Appl. Catal. B Environ. 239 (2018) 133–146. https://doi.org/10.1016/J.APCATB.2018.07.064.

[45] S. Choe, B.-S. Lee, M.K. Cho, H.-J. Kim, D. Henkensmeier, S.J. Yoo, J.Y. Kim, S.Y. Lee, H.S. Park, J.H. Jang, Electrodeposited IrO2/Ti electrodes as durable and cost-effective anodes in high-temperature polymer-membrane-electrolyte water electrolyzers, Appl. Catal. B Environ. 226 (2018) 289–294. https://doi.org/10.1016/J.APCATB.2017.12.037.

[46] C. Rozain, E. Mayousse, N. Guillet, P. Millet, Influence of iridium oxide loadings on

the performance of PEM water electrolysis cells: Part I–Pure IrO2-based anodes, Appl. Catal. B Environ. 182 (2016) 153–160. https://doi.org/10.1016/J.APCATB.2015.09.013.

[47] S. Siracusano, V. Baglio, N. Van Dijk, L. Merlo, A.S. Aricò, Enhanced performance and durability of low catalyst loading PEM water electrolyser based on a short-side chain perfluorosulfonic ionomer, Appl. Energy. 192 (2017) 477–489. https://doi.org/10.1016/J.APENERGY.2016.09.011.

[48] N. Giordano, E. Passalacqua, L. Pino, A.S. Arico, V. Antonucci, M. Vivaldi, K. Kinoshita, Analysis of platinum particle size and oxygen reduction in phosphoric acid, Electrochim. Acta. 36 (1991) 1979–1984. https://doi.org/10.1016/0013-4686(91)85082-I.

[49] A. Stassi, I. Gatto, V. Baglio, E. Passalacqua, A.S. Aricò, Oxide-supported PtCo alloy catalyst for intermediate temperature polymer electrolyte fuel cells, Appl. Catal. B Environ. 142–143 (2013) 15–24. https://doi.org/10.1016/j.apcatb.2013.05.008.

[50] S. Siracusano, N. Hodnik, P. Jovanovic, F. Ruiz-Zepeda, M. Šala, V. Baglio, A.S. Aricò, New insights into the stability of a high performance nanostructured catalyst for sustainable water electrolysis, Nano Energy. 40 (2017) 618–632. https://doi.org/10.1016/j.nanoen.2017.09.014.

Supplementary Materials

Click here to download Supplementary Materials: Supplementary Data.docx